Molecular Biology of the Cell
Vol. 11, 773–793, February 2000

Identification of Novel, Evolutionarily Conserved Cdc42p-interacting Proteins and of Redundant Pathways Linking Cdc24p and Cdc42p to Actin Polarization in Yeast

Erfei Bi,*† John B. Chiavetta,*‡ Herman Chen,* Guang-Chao Chen,§ Clarence S. M. Chan,§ and John R. Pringle*‖

*Department of Biology and Program in Molecular Biology and Biotechnology, University of North Carolina, Chapel Hill, North Carolina 27599; and §Section of Molecular Genetics and Microbiology and Institute for Cellular and Molecular Biology, University of Texas, Austin, Texas 78712

Submitted July 22, 1999; Revised November 24, 1999; Accepted December 8, 1999
Monitoring Editor: Tim Stearns

In the yeast *Saccharomyces cerevisiae,* Cdc24p functions at least in part as a guanine-nucleotide-exchange factor for the Rho-family GTPase Cdc42p. A genetic screen designed to identify possible additional targets of Cdc24p instead identified two previously known genes, *MSB1* and *CLA4*, and one novel gene, designated *MSB3,* all of which appear to function in the Cdc24p–Cdc42p pathway. Nonetheless, genetic evidence suggests that Cdc24p may have a function that is distinct from its Cdc42p guanine-nucleotide-exchange factor activity; in particular, overexpression of *CDC42* in combination with *MSB1* or a truncated *CLA4* in cells depleted for Cdc24p allowed polarization of the actin cytoskeleton and polarized cell growth, but not successful cell proliferation. *MSB3* has a close homologue (designated *MSB4*) and two more distant homologues (*MDR1* and *YPL249C*) in *S. cerevisiae* and also has homologues in *Schizosaccharomyces pombe, Drosophila* (*pollux*), and humans (the oncogene *tre17*). Deletion of either *MSB3* or *MSB4* alone did not produce any obvious phenotype, and the *msb3 msb4* double mutant was viable. However, the double mutant grew slowly and had a partial disorganization of the actin cytoskeleton, but not of the septins, in a fraction of cells that were larger and rounder than normal. Like Cdc42p, both Msb3p and Msb4p localized to the presumptive bud site, the bud tip, and the mother-bud neck, and this localization was Cdc42p dependent. Taken together, the data suggest that Msb3p and Msb4p may function redundantly downstream of Cdc42p, specifically in a pathway leading to actin organization. From previous work, the *BNI1, GIC1,* and *GIC2* gene products also appear to be involved in linking Cdc42p to the actin cytoskeleton. Synthetic lethality and multicopy suppression analyses among these genes, *MSB*, and *MSB4,* suggest that the linkage is accomplished by two parallel pathways, one involving Msb3p, Msb4p, and Bni1p, and the other involving Gic1p and Gic2p. The former pathway appears to be more important in diploids and at low temperatures, whereas the latter pathway appears to be more important in haploids and at high temperatures.

INTRODUCTION

A central feature of morphogenesis in many types of cells is cell polarization, which involves the asymmetric organization of the cytoskeleton, secretory system, and plasma membrane components along an appropriate axis (Drubin and Nelson, 1996). A protein of central importance in cell polarization is Cdc42p, a member of the Rho/Rac family of Ras-related small GTPases (Valencia *et al.*, 1991). Cdc42p was first identified in yeast by analysis of a temperature-sensitive mutant that was defective in cell polarization and bud emergence and thus formed large, round, isotropically growing cells at restrictive temperature (Pringle and Hartwell, 1981; Adams and Pringle, 1984; Pringle *et al.*, 1986; Adams *et al.*, 1990; Johnson and Pringle, 1990). It was subsequently found to be remarkably highly conserved (≥76% identical in amino acid sequence) in other types of eukaryotic cells, including humans (Johnson, 1999). In both yeast and animal cells,

† Present addresses: Department of Cell and Developmental Biology, University of Pennsylvania, Philadelphia, PA 19104-6058; ‡ School of Medicine, University of North Carolina, Chapel Hill, NC 27599.
‖ Corresponding author. E-mail address: jpringle@email.unc.edu.
Abbreviations used: CRIB domain, Cdc42/Rac-interactive-binding domain; DIC, differential interference contrast; FH, formin homology; FITC, fluorescein isothiocyanate; GAP, GTPase-activating protein; GEF, guanine-nucleotide-exchange factor; GFP, green fluorescent protein; 3HA, triple hemagglutinin epitope; IgG, immunoglobulin G; PAK, p21-activated kinase; PH domain, pleckstrin-homology domain.

Table 1. *Saccharomyces cerevisiae* strains used in this study

Strain	Genotype	Reference or source
YEF473	**a**/α *his3/his3 leu2/leu2 lys2/lys2 trp1/trp1 ura3/ura3*	Bi and Pringle, 1996
YEF473A	**a** *his3 leu2 lys2 trp1 ura3*	Segregant from YEF473
YEF473B	α *his3 leu2 lys2 trp1 ura3*	Segregant from YEF473
YEF313	**a** *ade2 his3 leu2 lys2 trp1 ura3 cdc24-4*	This study[a]
YEF316	**a** *ade2 his3 leu2 lys2 trp1 ura3 cdc24-10*	Bi and Pringle, 1996
YEF319	α *ade2 his3 his4 leu2 lys2 trp1 ura3 cdc24-11*	This study[a]
YEF323	α *ade2 his4 leu2 trp1 ura3 cdc24-12*	Bi and Pringle, 1996
YEF327	α *ade2 his4 leu2 trp1 ura3 cdc24-13*	Bi and Pringle, 1996
DJTD2-16D	α *gal2 his4 leu2 trp1 ura3 cdc42-1*	Johnson and Pringle, 1990
YEF1234	as YEF473 except *MSB3/msb3*Δ*::HIS3*	See text
YEF1239	**a** *his3 leu2 lys2 trp1 ura3 msb3*Δ*::HIS3*	Segregant from YEF1234
YEF1242	α *his3 leu2 lys2 trp1 ura3 msb3*Δ*::HIS3*	Segregant from YEF1234
YEF1292	as YEF473 except *MSB3/msb3*Δ*::TRP1*	See text
YEF1303	**a** *his3 leu2 lys2 trp1 ura3 msb3*Δ*::TRP1*	Segregant from YEF1292
YEF1235	as YEF473 except *MSB4/msb4*Δ*::HIS3*	See text
YEF1247	α *his3 leu2 lys2 trp1 ura3 msb4*Δ*::HIS3*	Segregant from YEF1235
YEF1249	**a** *his3 leu2 lys2 trp1 ura3 msb4*Δ*::HIS3*	Segregant from YEF1235
YEF1236	as YEF473 except *MSB4/msb4*Δ*::TRP1*	See text
YEF1256	**a** *his3 leu2 lys2 trp1 ura3 msb4*Δ*::TRP1*	Segregant from YEF1236
YEF1258	α *his3 leu2 lys2 trp1 ura3 msb4*Δ*::TRP1*	Segregant from YEF1236
YEF1293	as YEF473 except *MDR1/mdr1*Δ*::HIS3*	See text
YEF1310	**a** *his3 leu2 lys2 trp1 ura3 mdr1*Δ*::HIS3*	Segregant from YEF1293
YEF1312	α *his3 leu2 lys2 trp1 ura3 mdr1*Δ*::HIS3*	Segregant from YEF1293
YEF1294	as YEF473 except *YPL249C/ypl249C*Δ*::HIS3*	See text
YEF1321	α *his3 leu2 lys2 trp1 ura3 ypl249C*Δ*::HIS3*	Segregant from YEF1294
YEF1295	as YEF473 except *YPL249C/ypl249C*Δ*::TRP1*	See text
YEF1329	**a** *his3 leu2 lys2 trp1 ura3 ypl249C*Δ*::TRP1*	Segregant from YEF1295
YEF1330	α *his3 leu2 lys2 trp1 ura3 ypl249C*Δ*::TRP1*	Segregant from YEF1295
YEF1269	**a** *his3 leu2 lys2 trp1 ura3 msb3*Δ*::HIS3 msb4*Δ*::HIS3*	Segregant from YEF1239 × YEF1247[b,c]
YEF1270	α *his3 leu2 lys2 trp1 ura3 msb3*Δ*::HIS3 msb4*Δ*::HIS3*	Segregant from YEF1239 × YEF1247[b]
YEF1289	**a** *his3 leu2 lys2 trp1 ura3 msb3*Δ*::HIS3 msb4*Δ*::TRP1*	Segregant from YEF1239 × YEF1258
YEF1291	α *his3 leu2 lys2 trp1 ura3 msb3*Δ*::HIS3 msb4*Δ*::TRP1*	Segregant from YEF1239 × YEF1258
YEF1631	as YEF473 except *msb3*Δ*::HIS3/msb3*Δ*::HIS3 msb4*Δ*::TRP1/msb4*Δ*::TRP1*	YEF1289 × YEF1291[d]
YEF1358	**a** *his3 leu2 lys2 trp1 ura3 msb3*Δ*::TRP1 mdr1*Δ*::HIS3*	Segregant from YEF1303 × YEF1312
YEF1360	**a** *his3 leu2 lys2 trp1 ura3 msb3*Δ*::HIS3 ypl249C*Δ*::TRP1*	Segregant from YEF1239 × YEF1330
YEF1362	**a** *his3 leu2 lys2 trp1 ura3 msb4*Δ*::TRP1 mdr1*Δ*::HIS3*	Segregant from YEF1256 × YEF1312
YEF1363	α *his3 leu2 lys2 trp1 ura3 msb4*Δ*::TRP1 mdr1*Δ*::HIS3*	Segregant from YEF1256 × YEF1312
YEF1364	**a** *his3 leu2 lys2 trp1 ura3 msb4*Δ*::HIS3 ypl249C*Δ*::TRP1*	Segregant from YEF1249 × YEF1330
YEF1366	**a** *his3 leu2 lys2 trp1 ura3 mdr1*Δ*::HIS3 ypl249C*Δ*::TRP1*	Segregant from YEF1310 × YEF1330
YEF1354	α *his3 leu2 lys2 trp1 ura3 msb3*Δ*::HIS3 msb4*Δ*::TRP1 mdr1*Δ*::HIS3*	Segregant from YEF1291 × YEF1310[b]
YEF1356	**a** *his3 leu2 lys2 trp1 ura3 msb3*Δ*::HIS3 msb4*Δ*::HIS3 ypl249C*Δ*::TRP1*	Segregant from YEF1270 × YEF1329[b]
YEF1389	α *his3 leu2 lys2 trp1 ura3 msb3*Δ*::TRP1 mdr1*Δ*::HIS3 ypl249C*Δ*::HIS3*	Segregant from YEF1358 × YEF1321[b]
YEF1390	**a** *his3 leu2 lys2 trp1 ura3 msb4*Δ*::TRP1 mdr1*Δ*::HIS3 ypl249C*Δ*::HIS3*	Segregant from YEF1362 × YEF1321[b]
YEF1393	α *his3 leu2 lys2 trp1 ura3 msb3*Δ*::HIS3 msb4*Δ*::TRP1 mdr1*Δ*::HIS3 ypl249C*Δ*::TRP1*	Segregant from YEF1360 × YEF1363[b,c]
YEF1474	as YEF473 except *msb3*Δ*::HIS3/msb3*Δ*::HIS3 ura3:URA3:3HA-MSB3/ura3:URA3:3HA-MSB3*	See text
YEF1475	as YEF473 except *msb4*Δ*::HIS3/msb4*Δ*::HIS3 ura3:URA3:3HA-MSB4/ura3:URA3:3HA-MSB4*	See text
YEF1517	**a** *his3 leu2 lys2 trp1 ura3 cdc42*Δ*::HIS3 ura3:URA3:GFP-CDC42*	See text
JF16	**a** *ade2 his3 leu2 lys2 trp1 ura3 bni1*Δ*::LEU2*	H. Fares and J.R. Pringle[e]
YJZ426	as YEF473A except *bni1*Δ*::HIS3*	J. Zahner and J.R. Pringle[f]
HH799	as YEF473 except *bni1*Δ*::HIS3/bni1*Δ*::HIS3*	J. Zahner and J.R. Pringle[f]
CCY1042-12B	α *his3 leu2 lys2 trp1 ura3 gic1-*Δ*1::LEU2 gic2-*Δ*2::TRP1*	This study[g]
CCY1024-19C	α *his3 leu2 trp1 ura3 gic1-*Δ*1::LEU2 gic2-1::HIS3*	Chen *et al.*, 1997a
YEF1662	**a**/α *his3/his3 leu2/leu2 lys2/lys2 trp1/trp1 ura3/ura3 gic1-*Δ*1::LEU2/gic1-*Δ*1::LEU2 gic2-*Δ*2::TRP1/gic2-*Δ*2::TRP1*	This study[h]
YEF933	as YEF473 except *BEM3/bem3*Δ*::HIS3*	See text

Table 1. *Continued*

Strain	Genotype	Reference or source
YEF992	**a** *his3 leu2 lys2 trp1 ura3 bem3*Δ::*HIS3*	Segregant from YEF933
YEF959	as YEF473 except *RGA1/rga1*Δ::*HIS3*	See text
YEF1000	α *his3 leu2 lys2 trp1 ura3 rga1*Δ::*HIS3*	Segregant from YEF959
YEF1203	α *his3 leu2 lys2 trp1 ura3 bem3*Δ::*HIS3 rga1*Δ::*HIS3*	Segregant from YEF992 × YEF1000[c]
YEF1206	**a** *his3 leu2 lys2 trp1 ura3 bem3*Δ::*HIS3 rga1*Δ::*HIS3*	Segregant from YEF992 × YEF1000[c]
YEF1223	as YEF473 except *bem3*Δ::*HIS3/bem3*Δ::*HIS3 rga1*Δ::*HIS3/rga1*Δ::*HIS3*	YEF1203 × YEF1206
YEF1265	as YEF473 except *bem3*Δ::*HIS3/bem3*Δ::*HIS3 rga1*Δ::*HIS3/rga1*Δ::*HIS3 CDC24/cdc24*Δ::*TRP1*	See text
YEF1154	as YEF473 except *CDC24/cdc24*Δ::*HIS3*	See text
YEF1201	**a** *his3 leu2 lys2 trp1 ura3 cdc24*Δ::*HIS3* [pMGF5]	This study[i]

[a] Derived by several crosses from the original *cdc24* mutant strains isolated in the screens described by Sloat *et al.* (1981) and Harris and Pringle (1991).

[b] The genotypes of these strains were inferred from the 2 His^+:2 His^- (and, for YEF1393, 2 Trp^+:2 Trp^-) segregation pattern in the appropriate tetrad.

[c] The genotypes of these strains were confirmed by outcrossing them to strain YEF473A or YEF473B.

[d] Constructed by crossing strain YEF1289 harboring plasmid YEplac-MSB3 to strain YEF1291 harboring plasmid YEp352, selecting diploids on SC−Leu−Ura plates, and then curing both plasmids.

[e] Strain YPH501 (Sikorski and Hieter, 1989) was transformed with a DNA fragment in which nearly all of the *BNI1* open reading frame had been replaced by *LEU2*; JF16 is a segregant from such a transformant.

[f] *bni1*Δ::*HIS3* is a complete deletion of the *BNI1* open reading frame constructed using the method of Baudin *et al.* (1993). Strain HH799 was constructed by mating YJZ426 and an isogenic α strain.

[g] Derived from strains described by Chen *et al.* (1997a).

[h] An **a** *MSB3 gic1*-Δ*1*::*LEU2 gic2*-Δ*2*::*TRP1* segregant from YEF1239 × CCY1042-12B was mated to CCY1042-12B.

[i] Strain YEF1154 was transformed with the low-copy *TRP1 GAL1-CDC24* plasmid pMGF5 (see Table 2), and a segregant containing both *cdc24*Δ::*HIS3* and pMGF5 was isolated on plates containing 2% glucose + 2% galactose.

Cdc42p appears to participate in a variety of signaling pathways, including those leading to polarization of the actin cytoskeleton and (at least in yeast) of the septins of the neck filaments (Adams and Pringle, 1984; Pringle *et al.*, 1986, 1995; Amatruda and Cooper, 1992; Cvrčková *et al.*, 1995; Li *et al.*, 1995; Van Aelst and D'Souza-Schorey, 1997; Hall, 1998; Aspenström, 1999; Johnson, 1999). Thus, it is important to define both the proteins that regulate Cdc42p activity and the proteins that serve as effectors for the various Cdc42p-mediated signaling pathways.

Intensive efforts during the past few years have resulted in considerable progress along these lines. For example, it seems clear that Cdc42p-family proteins are activated by members of the Dbl family of guanine-nucleotide-exchange factor (GEF) proteins (Cerione and Zheng, 1996; Whitehead *et al.*, 1997), represented in yeast by Cdc24p (Hartwell *et al.*, 1974; Sloat *et al.*, 1981; Adams and Pringle, 1984; Zheng *et al.*, 1994b), and that their return to the GDP-bound state involves the action of specific GTPase-activating proteins (GAPs) (Lamarche and Hall, 1994), which in yeast include Bem3p (Zheng *et al.*, 1994b) and Rga1p/Dbm1p (Stevenson *et al.*, 1995; Chen *et al.*, 1996). The activity of yeast Cdc42p may also be regulated both by Rdi1p, a GDP-dissociation inhibitor (Koch *et al.*, 1997), and by the still-mysterious Zds1p and Zds2p proteins (Bi and Pringle, 1996).

In addition, many candidate Cdc42p effectors have been identified in yeast and other organisms. These include the p21-activated (PAK) family of protein kinases (Sells and Chernoff, 1997), represented in yeast by Ste20p, Cla4p, and Skm1p (Cvrčková *et al.*, 1995; Simon *et al.*, 1995; Zhao *et al.*, 1995; Peter *et al.*, 1996; Benton *et al.*, 1997; Leberer *et al.*, 1997; Martín *et al.*, 1997; Eby *et al.*, 1998); the Wiscott–Aldrich syndrome protein (WASP) family (Bi and Zigmond, 1999), represented in yeast by Las17p/Bee1p (Li, 1997; Naqvi *et al.*, 1998); the formin homology (FH) domain proteins (Frazier and Field, 1997; Wasserman, 1998), represented in yeast by Bni1p and Bnr1p (Jansen *et al.*, 1996; Zahner *et al.*, 1996; Evangelista *et al.*, 1997; Imamura *et al.*, 1997; Fujiwara *et al.*, 1998; Umikawa *et al.*, 1998); the IQGAPs (Machesky, 1998), represented in yeast by Iqg1p/Cyk1p (Epp and Chant, 1997; Lippincott and Li, 1998; Osman and Cerione, 1998; Shannon and Li, 1999); and phosphoinositide 3-kinase (Zheng *et al.*, 1994a). Many of these proteins share a conserved Cdc42p/Rac-interactive-binding (CRIB) domain (Burbelo *et al.*, 1995), and recent studies in yeast have identified additional CRIB domain proteins, Gic1p and Gic2p, as functionally redundant Cdc42p effectors that are involved in the polarization of the actin cytoskeleton (Brown *et al.*, 1997; Chen *et al.*, 1997a).

Despite this progress, it seems likely that additional Cdc42p-interacting proteins remain to be identified, and the details of the Cdc42p effector pathways remain poorly understood. Indeed, in some cases, such as the question of whether the PAK kinases are involved in actin polarization, the available data appear contradictory (Cvrčková *et al.*, 1995; Leberer *et al.*, 1997; Peter *et al.*, 1996; Benton *et al.*, 1997; Sells and Chernoff, 1997; Van Aelst and D'Souza-Schorey, 1997; Eby *et al.*, 1998; Hall, 1998; Johnson, 1999). In other cases, such as that of the yeast Msb1p protein (Bender and Pringle, 1989, 1991; Mack *et al.*, 1996), the available data

Table 2. Plasmids used in this study

Plasmid	Characteristics	Reference or source
YEp13	High-copy (2 μm), *LEU2*	Rose and Broach, 1991
YEp24	High-copy (2 μm), *URA3*	Rose and Broach, 1991
YEp352	High-copy (2 μm), *URA3*	Hill *et al.*, 1986
YEplac181	High-copy (2 μm), *LEU2*	Gietz and Sugino, 1988
YIplac211	Integrative vector, *URA3*	Gietz and Sugino, 1988
pSM217	High-copy (2 μm), *URA3*	Chen *et al.*, 1997b
pPB191	*MSB1* in YEp24	Bender and Pringle, 1991
YEp352-CLA4	*CLA4* in YEp352	F. Cvrčková[a]
pMGF5	*CDC24* under *GAL1* promoter control in a low-copy (*CEN*), *TRP1* vector	Miyamoto *et al.*, 1991
YEp352-CDC42	*CDC42* in YEp352	See text
YEp13-MSB1	Full-length *MSB1* in YEp13	See text
YEp13-CLA4*	A truncated *CLA4* in YEp13	See text
YEp352-42CLA4*	*CDC42* and the truncated *CLA4* in YEp352	See text
YEp13-MSBX	A plasmid from the YEp13 genomic library that carries three ORFs	See text
YEplac-MSB3	*MSB3* from YEp13-MSBX subcloned into YEplac181	See text
YEplac-MSB3D	A derivative of YEplac-MSB3 with an internal deletion in *MSB3*	See text
YEplac-ORF1/2	*YNL295W* and *YNL294C* from YEp13-MSBX subcloned into YEplac181	See text
YEplac-MSB4	PCR-amplified *MSB4* cloned in YEplac181	See text
YEplac-3HA-MSB3	*3HA-MSB3* in YEplac181	See text
YEplac-3HA-MSB4	*3HA-MSB4* in YEplac181	See text
pCC1107	High-copy (2 μm), *URA3*, *MSB3*	See text
pCC1108	High-copy (2 μm), *URA3*, *MSB4*	See text
pCC904	High-copy (2 μm), *URA3*, *GIC1*	See text
pCC967	High-copy (2 μm), *URA3*, *GIC2*	See text

[a] Derived from plasmids described by Cvrčková *et al.* (1995).

strongly suggest an interaction with Cdc42p, but there are as yet no good clues to the function of this interaction.

Another important question is whether the Dbl-family proteins have roles in addition to the activation of Cdc42p. In the case of Cdc24p, the Dbl homology domain that is implicated in its Cdc42p GEF activity comprises only ~200 of its 854 amino acids (Miyamoto *et al.*, 1991; Cerione and Zheng, 1996; Whitehead *et al.*, 1997; Aghazadeh *et al.*, 1998; Liu *et al.*, 1998; Soisson *et al.*, 1998). Although regions in the COOH-terminal portion of Cdc24p appear to be responsible for its binding of the bud-site-selection protein Rsr1p/Bud1p (Park *et al.*, 1997) and of the suspected scaffold protein Bem1p (Peterson *et al.*, 1994), the function(s) of other regions, including the NH_2-terminal ~290 amino acids, the pleckstrin-homology (PH) domain (Bender and Pringle, 1995; Cerione and Zheng, 1996), and the putative Ca^{2+}-binding sites (Ohya *et al.*, 1986; Miyamoto *et al.*, 1991; Bender and Pringle, 1995), remain unknown and might involve interactions with targets other than Cdc42p. Such targets might include additional Rho-type GTPases (Hart *et al.*, 1994; Horii *et al.*, 1994; Cid *et al.*, 1995; Tanaka and Takai, 1998) or other types of proteins. In the study reported here, we undertook genetic screens that were designed to identify such other hypothetical targets of Cdc24p. However, the genes identified all encode proteins that appear to function in conjunction with Cdc42p. The one novel gene identified, *MSB3*, along with its homologue *MSB4*, defines a pathway that appears to function redundantly with that involving Gic1p and Gic2p in the control of actin polarization. Although our studies failed to identify specific additional targets of Cdc24p, they did provide additional indirect evidence suggesting that such targets may exist.

MATERIALS AND METHODS

Strains, Growth Conditions, and Genetic and Recombinant DNA Methods

Yeast strains used in this study are listed in Table 1; the construction of strains containing deletions and/or tagged genes is described below. Cells were grown on YM-P or YPD rich liquid medium, solid YPD medium, or selective media (Lillie and Pringle, 1980; Guthrie and Fink, 1991), as indicated; 2% glucose was used as carbon source except where noted. Where noted, 1 M sorbitol was added to solid media to enhance the suppression of Ts^- phenotypes (Bender and Pringle, 1989), or 1 μg/ml 5-fluoroorotic acid (Toronto Research Chemicals, North York, Ontario, Canada) was added to select for the loss of *URA3*-containing plasmids (Sikorski and Boeke, 1991). *Escherichia coli* strain DH12S (Life Technologies, Gaithersburg, MD) was used routinely as a plasmid host. *E. coli* strain MC1066a (*leuB600 trpC9830 pytF74::Tn5 Kan^r ara hsdR hsdM$^+$ srl::Tn10 recA13*) was used to select plasmids carrying the yeast *LEU2* gene (Sandbaken and Culbertson, 1988). *E. coli* was grown under standard conditions (Sambrook *et al.*, 1989).

Standard methods of yeast genetics and recombinant DNA manipulation (Sambrook *et al.*, 1989; Guthrie and Fink, 1991) were used except where noted. Enzymes were purchased from New England Biolabs (Beverly, MA), and oligonucleotide primers were from Integrated DNA Technologies (Coralville, IA). For physical mapping, ^{32}P-labeled DNA fragments were used to probe a filter carrying the ordered set of λ′ clones of yeast genomic DNA (Riles *et al.*, 1993; American Type Culture Collection, Rockville, MD).

Plasmids

Plasmids used in this study are listed in Table 2 or described where appropriate below. Plasmid YEp352-CDC42 was constructed by subcloning an ~1.7-kb *Bam*HI–*Hin*dIII fragment that carries *CDC42* from YEp351-CDC42 (Ziman *et al.*, 1991) into the corresponding sites of YEp352. The genomic DNA library contains yeast *Sau*3A fragments inserted at the *Bam*HI site of YEp13 (DeMarini *et al.*, 1997). Plasmids YEp13-MSB1, YEp13-CLA4*, and YEp13-MSBX were isolated from this library in the genetic selection described below. Plasmid pEWP1 was constructed by subcloning an ~2.9-kb *CLA4**-carrying *Hin*dIII–*Sal*I fragment (both sites from the vector) from YEp13-CLA4* into the corresponding sites of pBluescript KS(+) (Stratagene, La Jolla, CA). Plasmid YEp352-42CLA4* was constructed by subcloning an ~2.5-kb *Eco*RI fragment (one site from the vector, the other from the insert, 1024 bp upstream of the *CLA4* start codon) from pEWP1 into the *Eco*RI site of YEp352-CDC42. Plasmid YEplac-MSB3 was constructed by subcloning an ~3.4-kb *Sac*I–*Bam*HI fragment (both sites from the insert) from YEp13-MSBX into the corresponding sites of YEplac181. Plasmid YEplac-MSB3D was constructed by deleting a 1238-bp *Bgl*II fragment internal to *MSB3* from YEplac-MSB3; this deletion results in an in-frame stop codon immediately downstream of the *Bgl*II site and thus eliminates the entire COOH terminus of Msb3p starting from codon 115. Plasmid YEplac-ORF1/2 was constructed by subcloning an ~4.1-kb *Hin*dIII fragment (one site from the vector, the other from the insert) from YEp13-MSBX into the *Hin*dIII site of YEplac181. Plasmid YEplac-MSB4 was constructed by cloning an ~3.9-kb PCR fragment into the *Eco*RI and *Xba*I sites of YEplac181, using corresponding sites that had been incorporated into primers MSB4-forward-2 and MSB4-reverse-2 (Table 3). The PCR reaction was carried out using the Expand long template PCR system (Boehringer Mannheim, Indianapolis, IN) and genomic DNA from strain YEF473 as template.

To construct plasmids encoding Msb3p tagged with a triple-hemagglutinin (3HA) epitope, the ~3.4-kb *Sac*I–*Bam*HI fragment from plasmid YEplac-MSB3 (see above) was cloned into the corresponding sites of pALTER-1 (Promega, Madison, WI). Using the protocol recommended by Promega and primer MSB3-*Not*I (Table 3), a *Not*I site was then introduced immediately downstream of the *MSB3* start codon. The ~3.4-kb *Sac*I–*Bam*HI fragment from the resulting plasmid was cloned into the corresponding sites of YIplac211, and a *Not*I fragment encoding the 3HA epitope (Tyers *et al.*, 1993) was cloned into the *Not*I site of the resulting plasmid, yielding plasmid YIplac-3HA-MSB3, which encodes an in-frame fusion of *3HA* and *MSB3*. The *Sac*I–*Sal*I fragment carrying *3HA-MSB3* from plasmid YIplac-3HA-MSB3 was then cloned into the corresponding sites of YEplac181, yielding plasmid YEplac-3HA-MSB3. Plasmids encoding a 3HA-tagged Msb4p were constructed similarly, using the ~3.9-kb *Eco*RI–*Xba*I fragment from YEplac-MSB4 (see above) and primer MSB4-*Not*I (Table 3); this yielded plasmids YIplac-3HA-MSB4 and YEplac-3HA-MSB4. A plasmid encoding a fusion of green fluorescent protein (GFP) to Cdc42p was constructed similarly, using the ~1.7-kb *Bam*HI–*Hin*dIII fragment carrying *CDC42* from YEp351-CDC42 (Ziman *et al.*, 1991), primer CDC42-*Not*I (Table 3), and a cassette encoding GFP (De Virgilio *et al.*, 1996); this yielded plasmid YIplac-GFP-CDC42.

To construct plasmid pCC1107, the ~3.4-kb *Sac*I–*Bam*HI fragment containing *MSB3* from YEplac-MSB3 was cloned into *Sac*I–*Bam*HI-digested pSM217. To construct plasmid pCC1108, the ~3.9-kb *Eco*RI–*Hin*dIII fragment containing *MSB4* from YEplac-MSB4 was cloned into *Eco*RI–*Hin*dIII-digested pSM217. To construct plasmid pCC904, the ~1.7-kb *Nco*I fragment containing *GIC1* (Chen *et al.*, 1997a) was blunt ended using T4 DNA polymerase and cloned into *Sma*I-digested pSM217. To construct plasmid pCC967, the ~3.1-kb *Eco*RI–*Bgl*II fragment containing *GIC2* (Chen *et al.*, 1997a) was cloned into *Eco*RI–*Bam*HI-digested pSM217.

Construction of Strains Containing Deletions and Tagged Genes

Complete deletions of the *MSB3, MSB4, MDR1, YPL249C, CDC42, BEM3, RGA1,* and *CDC24* coding regions were constructed using the PCR method described by Baudin *et al.* (1993). A pair of hybrid primers (Table 3) was used in each PCR reaction. The 5′-ends of the primers corresponded to sequences immediately upstream or downstream of the coding region to be deleted, whereas the 3′-ends of the primers corresponded to vector sequences flanking either *HIS3* or *TRP1* in plasmid pRS303 or pRS304 (Sikorski and Hieter, 1989), respectively. The amplified fragments were transformed into strain YEF473, selecting stable His^+ or Trp^+ transformants. The success of the deletion constructions was confirmed by PCR using a forward primer (Table 3) that corresponded to sequences upstream of the particular coding region and a reverse primer that was the same as the one used in making the deletion. In addition, a complete deletion of *CDC24* was constructed by transforming strain YEF1223 with a construct carrying the *TRP1* marker (generated by PCR as described above), yielding strain YEF1265. The success of this construction was confirmed by Southern blot analysis.

Strains expressing 3HA-tagged Msb3p, 3HA-tagged Msb4p, and GFP-tagged Cdc42p were constructed as follows. Plasmid YIplac-3HA-MSB3 (see above) was linearized within *URA3* with *Apa*I and transformed into strains YEF1239 and YEF1242, selecting for stable Ura^+ transformants, which were then mated to generate strain YEF1474. Similarly, plasmid YIplac-3HA-MSB4 was linearized within *URA3* with *Nco*I and transformed into strains YEF1247 and YEF1249, and the resulting Ura^+ transformants were mated to yield strain YEF1475. To construct strain YEF1517, one copy of *CDC42* was deleted in strain YEF473, using the PCR method as described above. The resulting strain was transformed with plasmid YIplac-GFP-CDC42 (see above) that had been linearized within *URA3* using *Eco*RV, and a segregant containing both the *cdc42* deletion and *GFP-CDC42* was selected.

Morphological Observations, Antibodies, and Protein Methods

Differential interference contrast (DIC) and fluorescence microscopy were performed using a Zeiss (Thornwood, NY) Axioskop or a Nikon (Garden City, NY) Microphot SA microscope with a 60× Plan-apo objective. Immunofluorescence and staining of chitin with Calcofluor were performed as described previously (Pringle, 1991; Pringle *et al.*, 1991) after fixing cells by adding formaldehyde directly to the culture medium (final concentration, 3.7%); bisBenzamide (Sigma, St. Louis, MO) was included in the immunofluorescence mounting medium to visualize DNA. Except where noted, actin rings and patches were visualized by staining cells with 20 U/ml rhodamine-conjugated phalloidin (Molecular Probes, Eugene, OR) for 5 or 30 min (Adams and Pringle, 1991).

The primary antibodies used included goat anti-actin antibodies (Karpova *et al.*, 1993); the rat monoclonal anti-tubulin antibody YOL1/34 (Kilmartin *et al.*, 1982; Kilmartin and Adams, 1984; Accurate Chemical and Scientific, Westbury, NY); rabbit polyclonal antibodies to Cdc11p (Ford and Pringle, 1991), Cdc24p (Pringle *et al.*, 1995; Park *et al.*, 1997), and Isp42p (Kassenbrock *et al.*, 1993); and the mouse monoclonal anti–HA-epitope antibody HA.11 (Berkeley Antibody Company, Richmond, CA). The secondary antibodies used included rhodamine-conjugated donkey anti-goat-immunoglobulin G (IgG), fluorescein isothiocyanate (FITC)-conjugated goat anti-rabbit-IgG, FITC-conjugated rat anti-mouse-IgG, rhodamine-conjugated goat anti-mouse-IgG, and FITC-conjugated goat anti-rat-IgG (all from Jackson ImmunoResearch Laboratories, West Grove, PA).

For immunoblot analysis, protein extracts were prepared by vortexing cells repeatedly with acid-washed glass beads (425–600 μm) in buffer (50 mM Tris-HCl, pH 7.5, 400 mM NaCl, 5 mM EDTA, 1% NP-40) containing a mixture of protease inhibitors (20 μg/ml phenylmethanesulfonyl fluoride, 1 μg/ml leupeptin, 1 μg/ml pepstatin

Table 3. Oligonucleotide primers used for gene deletion, cloning, and tagging

Name of primer	Sequence of primer
Primers used for PCR-mediated deletions[a]	
MSB3-forward	GGAGTCAAAGAGTTGCGCACCCAGAACCATTGTAATTAGCGATTGTACTGAGAGTGCACC
MSB3-reverse	ACATATTTGTTTATGCAAAAACAAAAACAGGAAGCAAAAGCTGTGCGGTATTTCACACCG
MSB4-forward	CACTTTTACAATCACAGAAGGCAAAACCCGGCATGACAGGGATTGTACTGAGAGTGCACC
MSB4-reverse	TTATTTTACACAGTTGCGCTTTTTATCACGGTTGCGCTTACTGTGCGGTATTTCACACCG
MDR1-forward	AACCTCAGAGTTGATACAATTATTAGTTAAAGGATAGGATGATTGTACTGAGAGTGCACC
MDR1-reverse	ACAGATGTTTTAGGGTGACATAAAATTGATAAGCACGATTCTGTGCGGTATTTCACACCG
YPL249C-forward	AGCTCCTACCACCAGTGTAAAGTAGAACGTTAATAGAGCAGATTGTACTGAGAGTGCACC
YPL249C-reverse	GGAGAGGCACACAATGTGCACACAGCGCAAAACTATACATCTGTGCGGTATTTCACACCG
CDC42-forward	CTCATAAAACAAGAAATAAACGTATTAGGTCTTCCACAAAGATTGTACTGAGAGTGCACC
CDC42-reverse	TAGATATAGATTAAGAAAAGATGGGCATATACTAATATGACTGTGCGGTATTTCACACCG
BEM3-forward	TATATTCTAGAATAAACTCACACTCAACTAACAGCACGCAGATTGTACTGAGAGTGCACC
BEM3-reverse	AGGTTTACTGGCAACGTTATATTTCTACAATTTTAGACCACTGTGCGGTATTTCACACCG
RGA1-forward	CTGATTCAGGTACTAGTGGTGGAGAGAGCGGCATATTAAAGATTGTACTGAGAGTGCACC
RGA1-reverse	AGTTCATATAAGGCGGCTCAATGCAGAACCGAGGATAGCGCTGTGCGGTATTTCACACCG
CDC24-forward	GCCCTATCAAGACCTGTCTGCTAATCCAACCCGAGAGATCGATTGTACTGAGAGTGCACC
CDC24-reverse	CTTGAATTATTTAGTATTTGCTGTATACTAGTTTTATTTACTGTGCGGTATTTCACACCG
Forward primers used for checking the deletions	
MSB3-check	AGGAGTCAAAGAGTTGCGCACCCAGAACCATTG
MSB4-check	TACAATCACAGAAGGCAAAACCCGGCATGACAG
MDR1-check	GAAAGCACTGATCCATCAATTAAAGCACCGAAC
YPL249C-check	TTGAGATTGATTAGTTAATACTCAAAATAAAAC
CDC42-check	CTGAGGAGATAGGTTAAC
BEM3-check	ACATCAGGCATATACAAC
RGA1-check	GTACAAGACAAGGATAGC
CDC24-check	GCAGAAGAGTACCATTGC
Primers used for cloning *MSB4*[b]	
MSB4-forward-2	ATCTGATAATATCCTTCTGAATTCCCAAGGGTTAGTGAAAAT
MSB4-reverse-2	AGACTCCTGAAACACAGGTCTAGAAAGAAGGGGCCCCAAAAC
Primers used for tagging with HA or GFP[c]	
MSB3-*Not*I	CCCAGAACCATTGTAATTAGCATGAGCGGCCGCCAGAACGATCAACAGAGGTTC
MSB4-*Not*I	AAAACCCGGCATGACAGGATGAGCGGCCGCATAATGTCATCAACTATGTCGACA
CDC42-*Not*I	TAGGTCTTCCACAAAATGAGCGGCCGCCAAACGCTAAAGTGTGTT

[a] The underlined sequences correspond to those immediately upstream or downstream of the coding region to be deleted. All sequences are written from 5′ to 3′.

[b] The *Eco*RI (MSB4-forward-2) and *Xba*I (MSB4-reverse-2) sites are underlined.

[c] The *Not*I sites are underlined.

A, 1 μg/ml aprotinin [all from Sigma]). The glass beads were allowed to settle, and the extracts were transferred to new tubes, diluted 1:1 with 5× SDS-lysis buffer (Laemmli, 1970), boiled for 10 min, and separated electrophoretically on a 10% SDS-polyacrylamide gel. Proteins were then transferred electrophoretically to nitrocellulose paper (Schleicher & Schuell, Keene, NH). Strips of nitrocellulose that carried different sizes of proteins were probed either with anti-Cdc24p or (as a loading control) with anti-Isp42p antibodies, using alkaline phosphatase–conjugated goat anti-rabbit-IgG (Jackson ImmunoResearch Laboratories) as secondary antibody.

RESULTS

Identification of a cdc24^{ts} Mutation that Is Not Suppressed by Multicopy CDC42

It is currently unclear whether Cdc24p has targets in addition to Cdc42p (see INTRODUCTION). We reasoned that if such additional targets exist, it might be possible to identify a *cdc24*^{ts} mutation that is not suppressed by multicopy *CDC42* alone but is suppressed by overexpression of the hypothetical target or by simultaneous overexpression of Cdc42p and the hypothetical target. Four previously isolated but incompletely characterized *cdc24*^{ts} mutants (carrying the alleles *cdc24-10*, *cdc24-11*, *cdc24-12*, and *cdc24-13*) were examined. Strains YEF316, YEF319, YEF323, and YEF327, along with the control strain YEF313 (*cdc24-4*), were transformed with plasmid YEp352-CDC42 and tested for growth at 37°C in the presence of 1 M sorbitol. Under these conditions, all of the *cdc24*^{ts} mutations but *cdc24-11* were suppressed, suggesting that the primary or exclusive defect caused by the mutations other than *cdc24-11* is in the GEF activity for Cdc42p. In contrast, although *cdc24-11* might only cause a more severe defect of the same type, it might also cause a defect in a distinct function (or functions) of Cdc24p and thus provide an opportunity to identify such a function genetically.

Isolation of Multicopy Suppressors of cdc24-11

In an initial attempt to identify such a distinct function by isolating multicopy suppressors of *cdc24-11*, strain YEF319

(*leu2 ura3 cdc24-11*) was transformed with a YEp13-based genomic DNA library. Transformants were plated on SC-Leu medium containing 1 M sorbitol and incubated at 37°C. Among ~45,000 transformants, 22 were found to have plasmid-dependent growth at 37°C. Twenty of these transformants also grew on SC-Leu plates without sorbitol at 37°C. Probing Southern blots of these 22 plasmids with a labeled *CDC24* fragment showed that they all carried *CDC24*, suggesting that no single gene on a high-copy plasmid, other than *CDC24* itself, can suppress the temperature-sensitive lethality of *cdc24-11*. The two plasmids that allowed growth only in the presence of sorbitol at 37°C presumably contained copies of *CDC24* that encoded proteins of lower activity or were expressed at a lower level.

If *cdc24-11* causes defects both in a Cdc42p-mediated function and in a second function of Cdc24p, it might be possible to suppress *cdc24-11* by simultaneous overexpression of *CDC42* and the gene mediating the second function. Thus, strain YEF319 harboring plasmid YEp352-CDC42 was transformed with the YEp13-based genomic DNA library, plated on SC-Leu-Ura medium, incubated overnight at 23°C (to allow transformants to recover), and shifted to 37°C for several days. One transformation plate was kept at 23°C to estimate the total number of transformants obtained. Transformants forming colonies at 37°C presumably contained multicopy plasmids that could suppress *cdc24-11* in the presence of YEp352-CDC42. Plasmids were recovered from these transformants into *E. coli* strain MC1066a (to select for the YEp13-based plasmids) and retransformed into strain YEF319 containing YEp352-CDC42 to confirm the suppression phenotype. Among ~92,000 transformants, 50 yielded plasmids that reproducibly allowed growth of the test strain on SC-Leu-Ura medium at 37°C.

Transformants containing these 50 plasmids were streaked on SC-Leu medium containing 5-fluoroorotic acid at 23°C to select for cells that had lost plasmid YEp352-CDC42. The resulting clones were streaked on SC-Leu medium with and without 1 M sorbitol at 37°C to test for suppression of *cdc24-11*. This divided the 50 suppressor plasmids into two classes. The first class contained 36 plasmids that allowed the *cdc24-11* mutant to grow at 37°C even in the absence of multicopy *CDC42*. With 18 of these plasmids, growth at 37°C was also sorbitol independent. Based on the results of the first multicopy suppressor screen with the *cdc24-11* allele (see above), these 18 plasmids were presumed to carry *CDC24* itself. The other 18 plasmids in this class also seemed likely to carry *CDC24* itself, and this was confirmed by Southern blot analyses. The second class contained 14 plasmids that did not suppress *cdc24-11* in the absence of YEp352-CDC42, even in the presence of 1 M sorbitol. These plasmids potentially identified genes that encode additional targets of Cdc24p.

The 14 plasmids were analyzed by restriction mapping and by probing Southern blots with labeled fragments of *CDC24*, *CDC42*, and *MSB1*. None was found to carry *CDC24* or *CDC42*. Twelve plasmids appeared to have overlapping inserts as judged by restriction mapping, and all 12 hybridized to the *MSB1* probe. In addition, the insert from one of these plasmids was shown to hybridize to λ′ clones (see MATERIALS AND METHODS) from the *MSB1* region; this plasmid was designated YEp13-MSB1. Sequencing and hybridization to the λ′ clones showed that one of the remaining two plasmids contained a truncated allele of *CLA4*; this plasmid was designated YEp13-CLA4*. Sequencing the ends of the insert DNA in the final plasmid and comparing these sequences to the genome database showed that the insert was derived from a region on the left arm of chromosome XIV not previously known to carry genes related in function to *CDC24* and *CDC42*. This plasmid was designated YEp13-MSBX.

*Suppression of cdc24 and cdc42 by MSB1 and CLA4**

To explore further the interactions among Msb1p, Cla4p, Cdc24p, and Cdc42p, we examined in detail the patterns of multicopy suppression. As indicated above, neither high-copy *CDC42* by itself (Figure 1A, sector 4) nor high-copy *MSB1* by itself (Figure 1A, sector 6) could suppress *cdc24-11* at 37°C, but the presence of both genes in high copy number resulted in good suppression (Figure 1A, sector 2). Similarly, high-copy *CLA4** by itself did not suppress *cdc24-11* (Figure 1A, sector 5), although it suppressed well in combination with high-copy *CDC42* (Figure 1A, sector 1). One possible explanation of these suppression patterns is that *cdc24-11* may be defective in two pathways, one involving *CDC42* and the other involving *MSB1* and/or *CLA4**. Consistent with this hypothesis is the observation that high-copy *MSB1* and *CLA4** together did not suppress *cdc24-11* in the absence of high-copy *CDC42* (Figure 1A, sector 3). However, it is also possible that *cdc24-11* is defective only in the Cdc42p-mediated pathway, but that high-copy *MSB1* or *CLA4** can somehow enhance the function of this pathway in the presence of high-copy *CDC42*. This latter hypothesis is supported by the observations that high-copy *MSB1* or *CLA4** alone suppressed *cdc42-1* well in the presence of 1 M sorbitol (Figure 1B, sectors 4 and 5) but did not suppress *cdc24-12* (Figure 1B, sectors 1 and 2) or several other *cdc24* alleles (our unpublished results) under the same conditions. Other evidence also supports the hypothesis that Msb1p and Cla4p are involved in the same pathway(s) as Cdc42p (see DISCUSSION).

Sequencing revealed that the truncated *CLA4** allele encodes a protein of 369 amino acids that lacks the entire kinase domain from the COOH-terminal half of the protein but has the PH and PAK domains in the NH_2-terminal region (Figure 1C). Interestingly, high-copy full-length *CLA4* (in plasmid YEp352-CLA4) did not suppress *cdc42-1* by itself and did not suppress *cdc24-11* in conjunction with high-copy *CDC42* (our unpublished results) (see DISCUSSION).

Suppression of cdc24 and cdc42 by MSB3

Plasmid YEp13-MSBX has an ~6.5-kb insert that contains three previously uncharacterized open reading frames (Figure 2A). Subcloning and deletion analysis showed that ORF *YNL293W* was responsible for the suppression of *cdc24-11* in conjunction with high-copy *CDC42* (Figure 2B). In the absence of high-copy *CDC42*, neither YEp13-MSBX nor YEplac-MSB3 (containing *YNL293W*) could suppress any of the *cdc24* alleles tested (*cdc24-4, cdc24-10, cdc24-11, cdc24-12,* and *cdc24-13*) at 37°C even in the presence of 1 M sorbitol (Figure 2C, sectors 1–4; our unpublished results). In contrast, YEp13-MSBX or YEplac-MSB3 alone could suppress *cdc42-1* efficiently at 37°C even in the absence of sorbitol (Figure 2C, sectors 5 and 6; our unpublished results). These

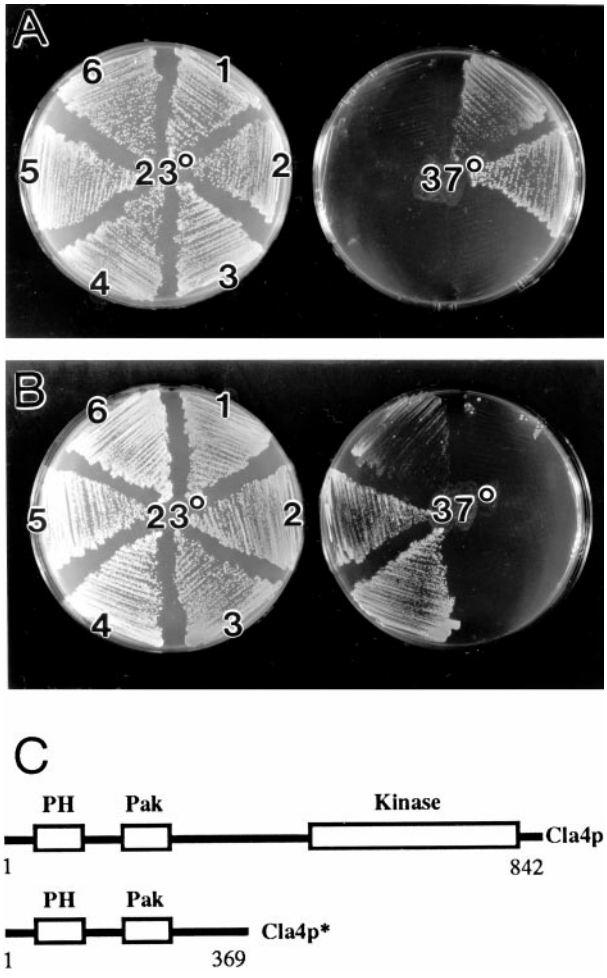

Figure 1. Suppression of *cdc24*^{ts} and *cdc42*^{ts} mutations by multicopy *MSB1* or multicopy truncated *CLA4*. The transformants described below were streaked onto SC-Leu-Ura plates with 1 M sorbitol (A) or SC-Leu plates with 1 M sorbitol (B) and incubated at the indicated temperatures. (A) *cdc24-11* strain YEF319 was transformed with (1) YEp352-CDC42 and YEp13-CLA4*, (2) YEp352-CDC42 and YEp13-MSB1, (3) YEp13-CLA4* and pPB191 (high-copy *MSB1*), (4) YEp352-CDC42 and YEp13, (5) YEp24 and YEp13-CLA4*, or (6) YEp24 and YEp13-MSB1. (B) *cdc24-12* strain YEF323 (1–3) and *cdc42-1* strain DJTD2–16D (4–6) were transformed with (3 and 6) YEp13, (2 and 5) YEp13-CLA4*, or (1 and 4) YEp13-MSB1. (C) Structures of full-length Cla4p and of the truncated Cla4p encoded by plasmid YEp13-CLA4*.

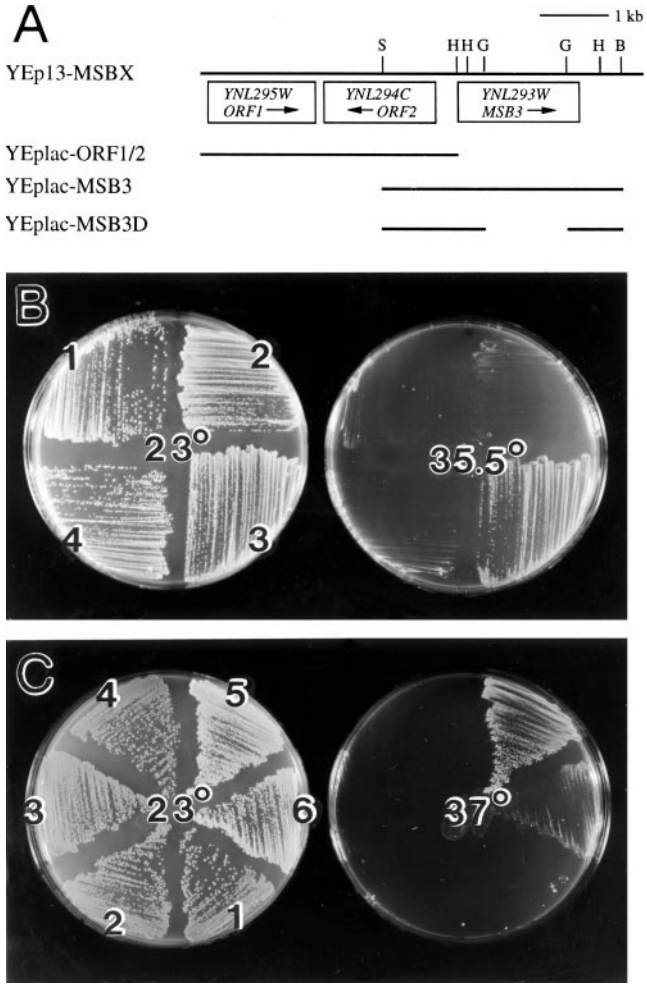

Figure 2. Suppression of *cdc24*^{ts} and *cdc42*^{ts} mutations by multicopy *MSB3*. (A) Physical maps of the inserts in plasmid YEp13-MSBX and in the subclones tested for suppression. All *Hin*dIII (H), *Sac*I (S), *Bgl*II (G), and *Bam*HI (B) sites are shown. (B and C) The transformants described below were streaked onto SC-Leu-Ura plates with 1 M sorbitol (B) or SC-Leu plates with 1 M sorbitol (C) and incubated at the indicated temperatures. (B) *cdc24-11* strain YEF319 harboring plasmid YEp352-CDC42 was transformed with (1) YEp13, (2) YEplac-MSB3D, (3) YEplac-MSB3, or (4) YEplac-ORF1/2. (C) *cdc24-13* strain YEF327 (1 and 2), *cdc24-12* strain YEF323 (3 and 4), and *cdc42-1* strain DJTD2–16D (5 and 6) were transformed with (2, 4, and 6) YEp13 or (1, 3, and 5) YEp13-MSBX.

observations suggest that Ynl293Wp, like Msb1p and Cla4p, is involved in the Cdc24p–Cdc42p pathway. By analogy with other genes identified as multicopy suppressors of budding defects, we designated *YNL293W* as *MSB3*.

Homology of Msb3p to Proteins from Yeast and Other Organisms

Database searches using the deduced amino acid sequence of Msb3p (633 amino acids) revealed that this protein belongs to a widely distributed family of proteins that share a homologous region of ~110 amino acids (Figure 3A). In addition to Msb3p, *Saccharomyces cerevisiae* contains three other members of this family, one of which, the ORF *YOL112W* gene product, is particularly closely related to Msb3p (51% sequence identity over its full 492 amino acids) and is thus designated Msb4p (Figure 3A). The other two *S. cerevisiae* family members, Mdr1p (950 amino acids; Serpe and Kosman, unpublished *Saccharomyces* Genome Database entry, 1996) and the product of ORF *YPL249C* (894 amino acids), are less closely related to Msb3p (Figure 3A). In addition, two members of this family have been identified in *Schizosaccharomyces pombe*, one in *Drosophila melanogaster*,

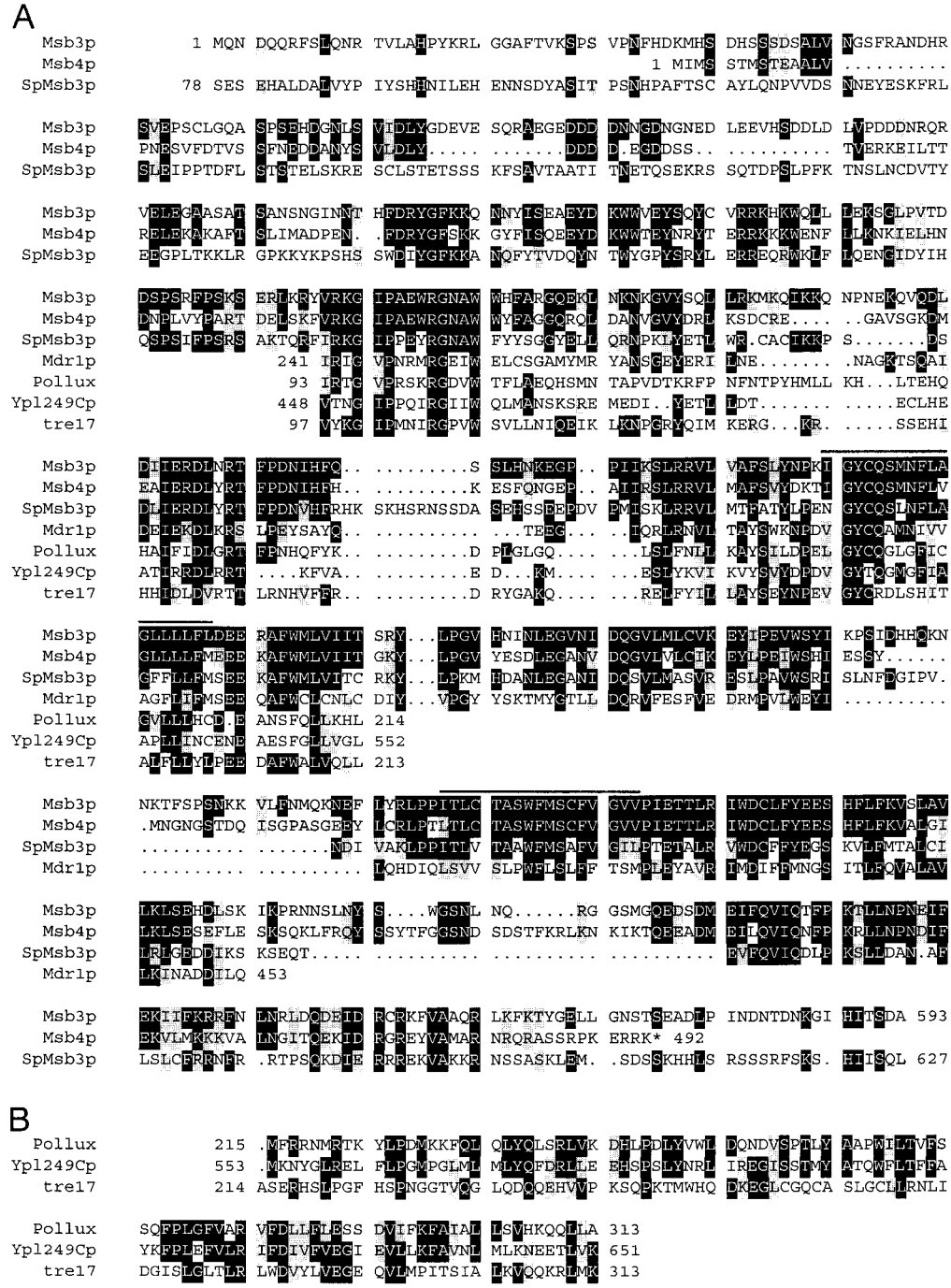

Figure 3. Alignment of Msb3p-homologous sequences from different organisms using the Genetics Computer Group (Madison, WI) Pile-Up program plus some manual adjustments. (A) The complete sequences of Msb3p, Msb4p, and SpMsb3p are shown except for the COOH terminus of Msb3p and the NH_2 and COOH termini of SpMsb3p; for the other proteins, only the regions of clear homology to Msb3p are shown (213 amino acids for Mdr1p; 105–122 amino acids for Pollux, Ypl249Cp, and tre17). Black boxes indicate amino acids identical to those in Msb3p; gray boxes indicate amino acids similar to those in Msb3p (D/E; Q/N; R/K; S/T; I/L/V). Overlining indicates the possible transmembrane domains (see text). The proteins depicted (with accession numbers) include the four proteins from *S. cerevisiae* (Msb3p [U23084], Msb4p [S51885], Mdr1p [Z72885], and Ypl249Cp [Z67751]); one from *S. pombe* (SpMsb3p [the product of a previously uncharacterized ORF on cosmid SPCC4G3 from chromosome III]); one from *D. melanogaster* (Pollux [U50542]); and one from *H. sapiens* (tre17 [S22155]). Other known proteins showing this region of homology include one from *S. pombe* (Z56276); seven from *C. elegans* (Z78539, U67954, Q09445, U49940, U42831, U41540, and U29244); one from *M. musculus* (Tbc1 [U33005]); and one from *H. sapiens* (D13644). (B) The sequences of Pollux, Ypl249Cp, and tre17 are shown for the region immediately downstream of the portions of these proteins shown in A. Black boxes indicate amino acids identical in two or more of the proteins; gray boxes indicate amino acids similar (as in A) in two or more of the proteins.

seven in *Caenorhabditis elegans*, one in *Mus musculus*, and two in *Homo sapiens* (Figure 3). One of the *S. pombe* proteins (here designated SpMsb3p; 635 amino acids) is highly homologous to Msb3p and Msb4p (35% sequence identity over the full-length proteins; 47–50% sequence identity over the central region of 310 amino acids), suggesting that the function(s) of Msb3p and Msb4p may be evolutionarily conserved. Thirteen amino acids are absolutely conserved among the seven sequences aligned in Figure 3A. Interestingly, Pollux, Ypl249Cp, and tre17 also share a region of homology with each other (although not with Msb3p, Msb4p, SpMsb3p, and Mdr1p) in a region immediately downstream from that in which all seven proteins are homologous (Figure 3B). Little is known about the function of this family of proteins (see DISCUSSION).

The program TM-pred (Hofmann and Stoffel, 1993) predicts two potential membrane-spanning domains in Msb3p (residues 320–337 and 424–440; indicated by overlining in Figure 3A), two in Msb4p (residues 238–255 and 335–351, corresponding to Msb3p 320–327 and 424–440), four in Mdr1p (residues 122–141, 326–343, 400–416, and 427–444, the middle two of which correspond to Msb3p 320–327 and 424–440), and two in Ypl249Cp (residues 561–576 and 595–612). The program of Lupas (1996) identifies one region in Msb3p (residues 236–270, $p = 0.35$) with some potential to form coiled coils and two regions in Ypl249Cp (residues 729–810, $p = 0.99$; residues 822–876, $p = 0.99$) with strong potential to form coiled coils. Potential coiled coils were not identified in Msb4p or Mdr1p. The functions of these regions remain to be determined.

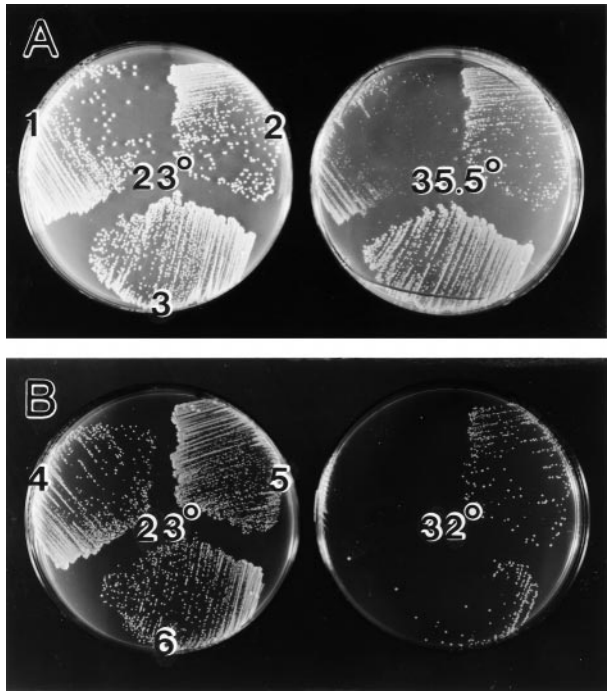

Figure 4. Suppression of *cdc24-11* by multicopy *MSB4*. Strain YEF319 with (A) or without (B) plasmid YEp352-CDC42 was transformed with plasmid YEp13 (1 and 4), YEplac-MSB4 (2 and 5), or YEplac-MSB3 (3 and 6). The transformants were streaked onto SC-Leu-Ura plates with 1 M sorbitol (A) or SC-Leu plates with 1 M sorbitol (B) and incubated at the indicated temperatures.

Functional Analysis of MSB3, MSB4, MDR1, and YPL249C

The similarity in sequence between Msb4p and Msb3p suggested that Msb4p might also interact with Cdc24p and/or Cdc42p. As one test of this hypothesis, we amplified *MSB4* by PCR and cloned it into a high-copy vector, generating plasmid YEplac-MSB4, which was then assayed for its ability to suppress *cdc24* and *cdc42* mutations. High-copy *MSB4* suppressed *cdc24-11* effectively in conjunction with high-copy *CDC42* at 35.5°C (Figure 4A, sector 2) and could even suppress *cdc24-11* weakly in the absence of high-copy *CDC42* at 32°C (Figure 4B, sector 5). However, unlike *MSB3*, high-copy *MSB4* failed to suppress *cdc42-1* (our unpublished results).

To explore further the functions of Msb3p and its homologues, we examined the phenotypic consequences of precise deletions of *MSB3*, *MSB4*, *MDR1*, and *YPL249C*, alone and in combination. None of the four single mutants displayed any obvious growth defect or morphological abnormalities at temperatures ranging from 23 to 37°C (Figure 5, A, sectors 2 and 3, C, and D; our unpublished results). Strains deleted for all four genes or any combination of two or three genes (see Table 1 for a list of strains constructed and examined) were viable over the same temperature range, indicating that these four genes are not essential for viability under laboratory conditions. However, the *msb3 msb4* double mutants (as well as the quadruple mutant and triple mutants containing both the *msb3* and *msb4* deletions) grew significantly more slowly than did the wild-type strain at 23°C (Figure 5A, sector 4; our unpublished results). In addition, nearly all of the *msb3 msb4* cells became rounder than normal (Figure 5E), and a fraction (15–20%) were larger than normal (Figure 5E), suggesting that there is a defect in the polarization of growth. This phenotype was not significantly enhanced by deletion of *MDR1*, *YPL249C*, or both, suggesting that although all four proteins share the conserved domain, Mdr1p and Ypl249Cp may function in a pathway(s) distinct from that involving Msb3p and Msb4p.

In *S. cerevisiae,* the actin cytoskeleton and the septins appear to polarize independently of each other, but both are dependent on Cdc42p (Adams and Pringle, 1984; Adams *et al.*, 1990; Ford and Pringle, 1991; Amatruda and Cooper, 1992; Cvrčková *et al.*, 1995; Li *et al.*, 1995; Pringle *et al.*, 1995; Ayscough *et al.*, 1997). To ask whether Msb3p and Msb4p are involved in the polarization of the actin cytoskeleton, the septins, or both, we stained cells of the *msb3 msb4* double mutant for F-actin and for Cdc11p. Actin appeared randomly distributed in the cell cortex in most, if not all, of the large, round cells of the double mutant (Figure 6D). About half of these cells contained two or more nuclei (Figure 6F, lower two cells). Interestingly, among the cells with disorganized actin, most (65 of 75 cells scored) had patterns of Cdc11p localization that appeared at least approximately normal (Figure 6E). These results suggest that Msb3p and Msb4p are involved in the control of actin organization, but not of septin organization, by Cdc42p.

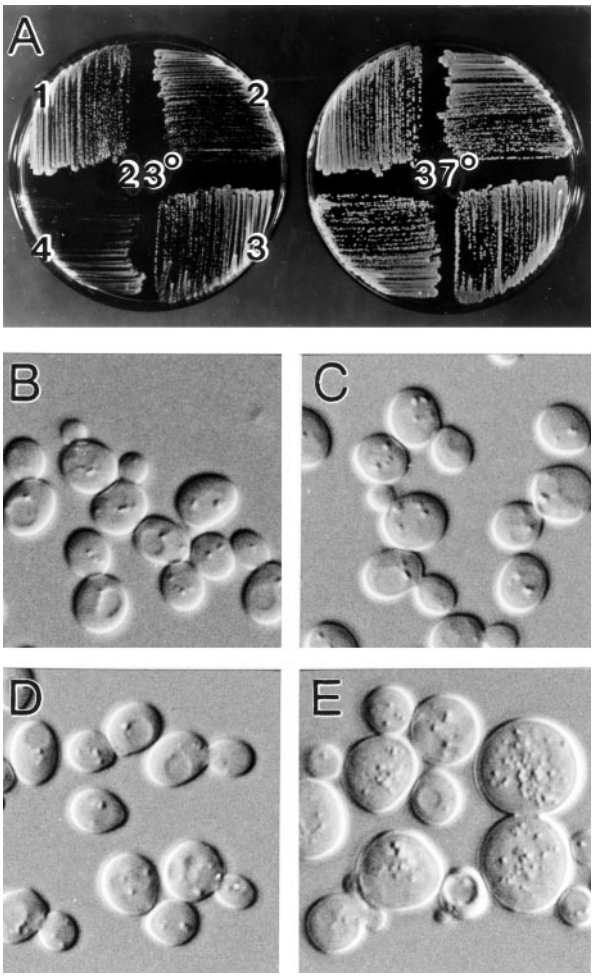

Figure 5. Phenotypic consequences of deleting *MSB3* and *MSB4*. (A) Growth of single and double mutants on YPD solid medium at 23 or 37°C. (B–E) Morphology of the single and double mutants in YPD liquid medium at 23°C, as observed by DIC microscopy. (A, sector 1, and B) YEF473A (wild-type); (A, sector 2, and C) YEF1239 (*msb3*Δ*::HIS3*); (A, sector 3, and D) YEF1247 (*msb4*Δ*::HIS3*); (A, sector 4, and E) YEF1269 (*msb3*Δ*::HIS3 msb4*Δ*::HIS3*). B–E are printed at the same magnification.

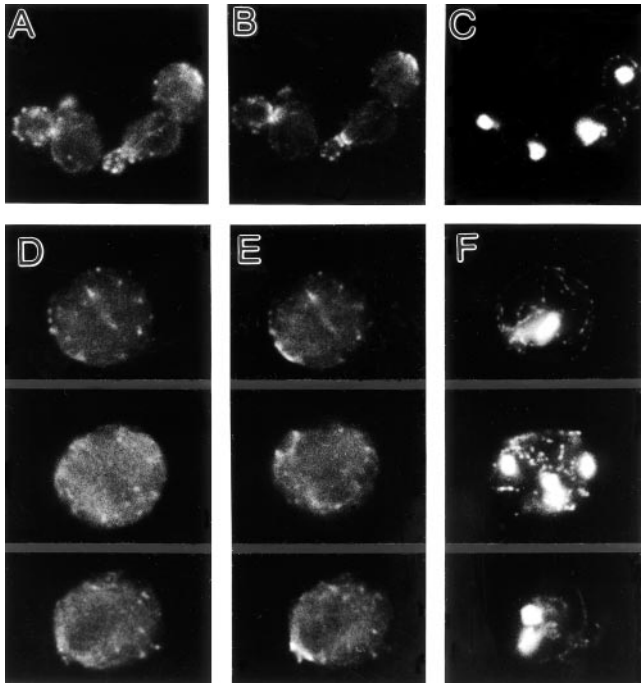

Figure 6. Actin and septin organization in the *msb3 msb4* double mutant. Cells of wild-type strain YEF473A (A–C) and *msb3 msb4* double-mutant strain YEF1269 (D–F) growing exponentially in YPD liquid medium at 23°C were triple stained for actin (A and D), Cdc11p (B and E), and DNA (C and F). All panels are printed at the same magnification.

Localization of Msb3p and Msb4p and Its Dependence on Cdc42p

To explore further the apparent functional interactions among Msb3p, Msb4p, and Cdc42p, we used HA-epitope–tagged Msb3p and Msb4p to localize these proteins. Both tagged genes on high-copy plasmids (low-copy plasmids were not tested) were able to complement the phenotypes of the double mutant, suggesting that the tagged genes are functional. Initial localization experiments used diploid strains (YEF1474 and YEF1475) that were homozygous for integrated single copies of *HA-MSB3* and *HA-MSB4*, respectively. Although immunofluorescence using anti-HA antibody allowed localization of the tagged Msb3p in some cells, the signal was very weak, and no signal was detected for the tagged Msb4p. Thus, strains YEF1474 and YEF1475 were transformed with high-copy plasmids (YEplac-3HA-MSB3 and YEplac-3HA-MSB4) containing *HA-MSB3* and *HA-MSB4*, respectively. Immunostaining of the transformants with anti-HA antibody yielded detectable signals for both proteins. In the case of Msb3p, this signal was stronger and more consistent than, but qualitatively similar to, the signal obtained with the untransformed strain.

In the transformed strains, HA-Msb3p and HA-Msb4p displayed similar patterns of localization through the cell cycle. Both proteins were first observed in unbudded cells at the presumptive bud site, as indicated by the consistent association with actin staining at the same site (Figure 7, A–C, cell 1; Figure 8, A–C, cell 1). In cells with small and medium-sized buds, Msb3p and Msb4p were localized to the bud tips (Figure 7, A–C, cell 2, and D and E, cell 1; Figure 8, A–C, cell 2). Later in the cell cycle, Msb3p and Msb4p became undetectable (Figure 7, A–C, cell 3, and D and E, cell 2; our unpublished results). The loss of the Msb3p and Msb4p signals from the bud tip occurred at approximately the same stage as the apical-to-isotropic shift (Lew and Reed, 1993) in actin organization and the extension of the mitotic spindle through the neck (Figure 7, A–C, cf. cell 2 to cell 3; Figure 7, D and E, cf. cell 1 to cell 2; our unpublished results). Among 46 cells showing localization of HA-Msb3p to the bud tip, 32 clearly had apically concentrated actin, whereas 14 appeared to have actin more isotropically arranged in the bud, and cells lacking an HA-Msb3p signal at the bud tip invariably displayed isotropically arranged actin. Near the end of the cell cycle, in cells with fully elongated spindles

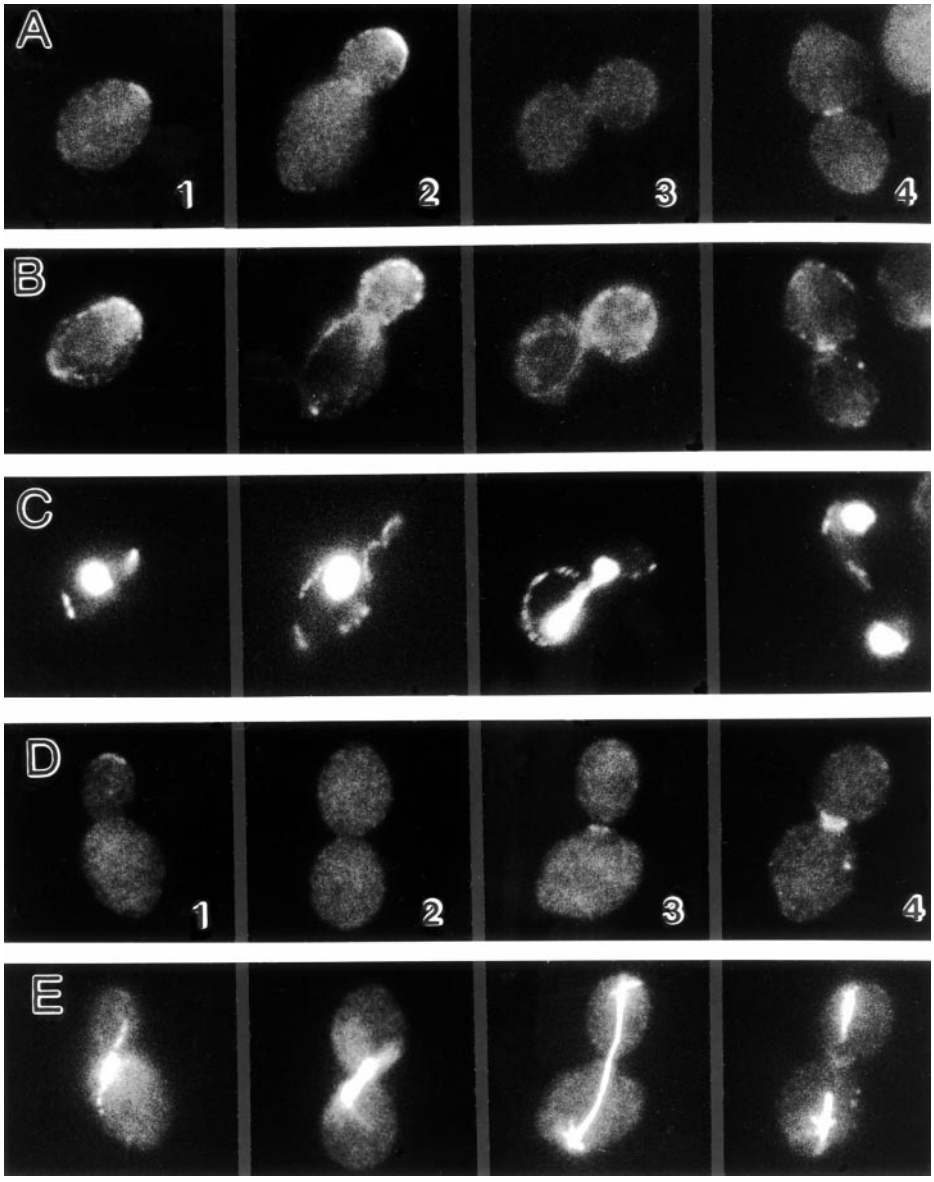

Figure 7. Immunolocalization of HA-tagged Msb3p. Cells of strain YEF1474 harboring plasmid YEplac-3HA-MSB3 growing exponentially in SC-Leu liquid medium at 23°C were triple stained for HA-tagged Msb3p (A), actin (B), and DNA (C) or double stained for HA-tagged Msb3p (D) and tubulin (E). Individual cells are numbered for reference in the text.

and well separated chromosome sets, HA-Msb3p and HA-Msb4p again became detectable but were now found in a single ring at the mother-bud neck (Figure 7, A–C, cell 4, and D and E, cell 3; Figure 8, A–C, cell 3) that was coincident (in 24 of 24 cells scored for Msb3p) with the ring of actin observed in such cells (Figures 7B, cell 4, and 8B, cell 3; also see Bi *et al.*, 1998; Lippincott and Li, 1998). Msb3p and Msb4p appeared to remain at the division site on both mother and daughter cells for some time after spindle breakdown and (presumably) cytokinesis (Figure 7, D and E, cell 4; our unpublished results); however, as very few unbudded cells were observed with two patches of HA-Msb3p or HA-Msb4p staining, these division-site remnants must disassemble before the new bud site is organized. The correlation between the localization of Msb3p and Msb4p and that of actin (see above) and Cdc42p (Ziman *et al.*, 1993; our unpublished results; see DISCUSSION) supports the hypothesis that Msb3p and Msb4p are involved in a pathway that links Cdc42p to the actin cytoskeleton (as discussed further below).

If this hypothesis is correct, it might also be predicted that the localization of Msb3p and Msb4p would depend on Cdc42p function. A difficulty in testing this hypothesis was that the *cdc42-1* mutation can be suppressed by multicopy *MSB3* (see above), including the multicopy *HA-MSB3* as used in the localization experiments. However, serendipitously, a strain carrying a *GFP-CDC42* allele (constructed for other purposes) was found to have a temperature-sensitive-lethal phenotype that was not suppressed by multicopy *MSB3*. When this strain (YEF1517) was transformed with YEplac-3HA-MSB3 or YEplac-3HA-MSB4 and grown at 23°C, Msb3p (Figure 8D), Msb4p (our unpublished results),

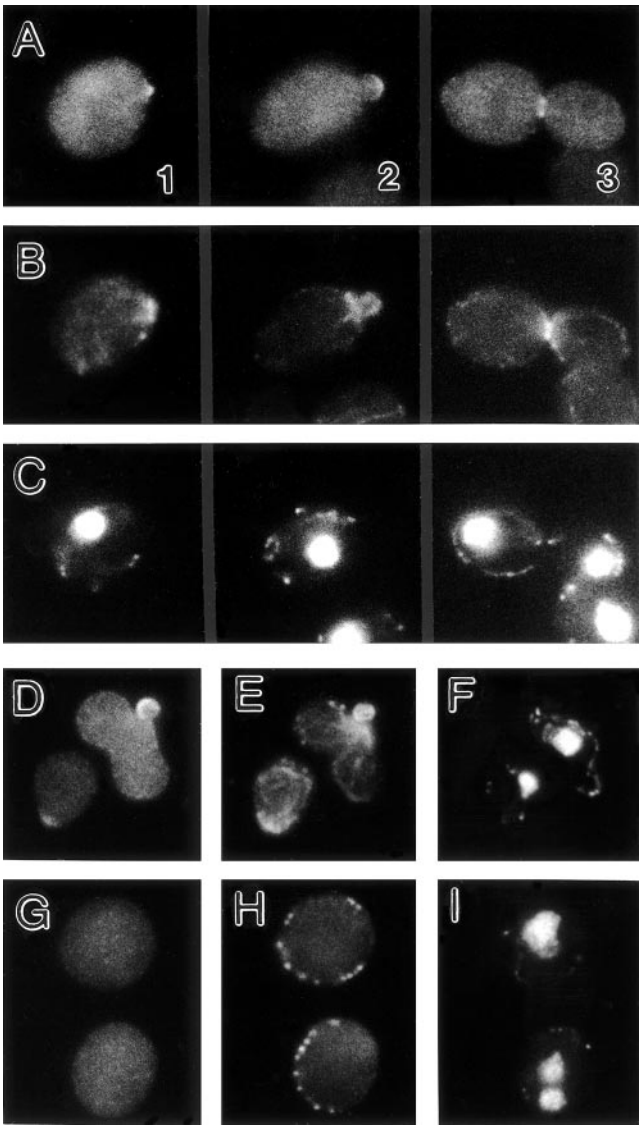

Figure 8. Immunolocalization of HA-tagged Msb4p (A–C) and dependence of Msb3p localization on Cdc42p (D–I). (A–C) Cells of strain YEF1475 containing plasmid YEplac-3HA-MSB4 growing exponentially in SC-Leu liquid medium at 23°C were triple stained for HA-tagged Msb4p (A), actin (B), and DNA (C). Individual cells are numbered for reference in the text. (D–I) Cells of strain YEF1517 (temperature-sensitive for Cdc42p function; see text) harboring plasmid YEplac-3HA-MSB3 growing exponentially in SC-Leu liquid medium at 23°C (D–F) or shifted to 37°C for 4 h (G–I) were triple stained for HA-tagged Msb3p (D and G), actin (E and H), and DNA (F and I).

and actin (Figure 8E) appeared to localize normally, although some cells were misshapen even at this temperature (e.g., the upper right cell in Figure 8D). However, after a shift to 37°C for 4 h, actin appeared to be randomly distributed in the cortex of the large, round cells (Figure 8H), and no Msb3p or Msb4p localization was observed (Figure 8G; our unpublished results). Similar results were obtained when the localization of 3HA-Msb4p was examined in a *cdc42-1* strain after 4 h at 37°C (our unpublished results). Thus, as predicted, the localization of Msb3p and Msb4p indeed appears to depend on Cdc42p.

Evidence for Parallel Pathways Linking Cdc42p to the Actin Cytoskeleton

If Msb3p and Msb4p are involved in linking Cdc42p to the actin cytoskeleton, why is the *msb3 msb4* double mutant viable? One possibility is that there are other proteins that have overlapping function or that constitute a parallel pathway. Evidence from other studies has suggested that Bni1p, Gic1p, and Gic2p may also be targets of Cdc42p that are involved in the organization of the actin cytoskeleton (Brown *et al.*, 1997; Chen *et al.*, 1997a; Evangelista *et al.*, 1997; Imamura *et al.*, 1997; see INTRODUCTION). Thus, we asked whether mutations in these genes are synthetically lethal with *msb3* and/or *msb4*, performing the experiments at 23°C. First, strain YEF1291 (α *msb3*Δ*::HIS3 msb4*Δ*::TRP1*) was crossed to strain JF16 (**a** *bni1*Δ*::LEU2*). Among 74 tetrads dissected, 68 produced four viable segregants, five produced three viable segregants, and one produced two viable segregants. Fourteen viable triple mutants (His^+ Trp^+ Leu^+) were recovered (the small number reflecting the linkage of *MSB3* and *BNI1* on the left arm of chromosome XIV), and none of the seven inviable segregants was predicted (from the genotypes of the other segregants in the same tetrad) to be a triple mutant. Thus, the *msb3*, *msb4*, and *bni1* mutations are not synthetically lethal. Next, strain YEF1269 (**a** *msb3*Δ*::HIS3 msb4*Δ*::HIS3*) was crossed to strain CCY1042-12B (α *gic1*-Δ*1::LEU2 gic2*-Δ*2::TRP1*), and 173 tetrads were dissected. Viable segregants were recovered that represented all of the possible double and triple mutants. However, 11% of the segregants were inviable, including all 19 that could be predicted unambiguously to harbor all four mutations. Moreover, when six viable His^+ Leu^+ Trp^+ segregants that might have been quadruple mutants were outcrossed to strain YEF473A or YEF473B, all six proved to be triple mutants (containing *msb3*Δ*::HIS3* or *msb4*Δ*::HIS3* but not both). Thus, the *msb3* and *msb4* mutations appear to be synthetically lethal in combination with the *gic1* and *gic2* mutations. Finally, strain YJZ426 (**a** *bni1*Δ*::HIS3*) was crossed to strain CCY1042-12B, and 20 tetrads were dissected. Of the 69 viable segregants, none was a triple mutant (although the three mutations should segregate independently), and 7 of the 11 inviable segregants could be predicted to be triple mutants. Thus, the *bni1* mutation appears to be synthetically lethal with the *gic1* and *gic2* mutations. For both the predicted *msb3 msb4 gic1 gic2* quadruple mutants and the predicted *bni1 gic1 gic2* triple mutants, microscopic examination of the inviable spore clones revealed microcolonies (one to a few cells) consisting almost entirely of large, round, unbudded cells. Taken together, the data suggest that Msb3p/Msb4p and Bni1p may be involved in one pathway linking Cdc42p to the actin cytoskeleton, whereas Gic1p/Gic2p may function in a second, parallel pathway.

If this hypothesis is correct, enhancing one signaling pathway might compensate for a defect in the other. Indeed, high-copy *MSB3* was found to suppress effectively the temperature-sensitive growth and morphological defects of the *gic1 gic2* double mutant (Figure 9, A and D), and high-copy *MSB4* also suppressed these defects, although somewhat less effectively (Figure 9, A and E). However, in the recip-

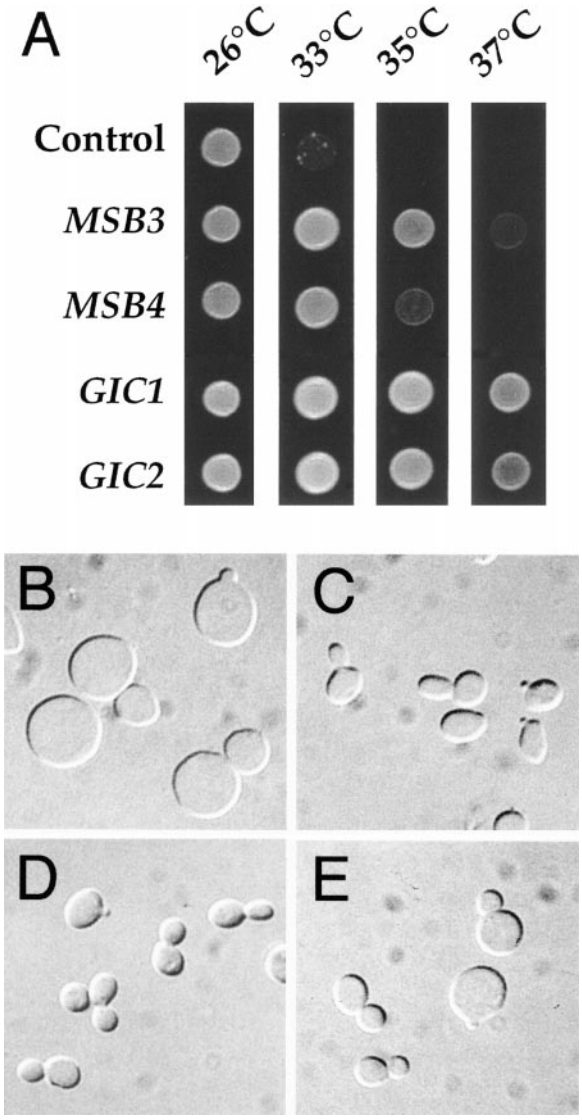

Figure 9. Suppression of the *gic1 gic2* double mutant by multicopy *MSB3* or *MSB4*. (A) Suspensions of strain CCY1024–19C harboring plasmid pSM217 (control), pCC1107 (*MSB3*), pCC1108 (*MSB4*), pCC904 (*GIC1*), or pCC967 (*GIC2*) were spotted on YPD plates and incubated for 2 days at the indicated temperatures. (B–E) Cells of strain CCY1024–19C containing plasmid pSM217 (B), pCC904 (C), pCC1107 (D), or pCC1108 (E) were grown to exponential phase in SD+Ade+Trp+casamino acids medium at 26°C and then shifted to 37°C for 4 h before fixation and examination by DIC microscopy. B–E are printed at the same magnification.

rocal experiment, high-copy *GIC1* or *GIC2* (plasmid pCC904 or pCC967) did not appear to suppress the growth and morphological defects of the *msb3 msb4* double-mutant strains YEF1269 and YEF1631 (our unpublished results; see DISCUSSION).

If Msb3p/Msb4p and Bni1p indeed function in one pathway while Gic1p/Gic2p function in another, then at least some of the phenotypes of the *msb3 msb4* double mutant should resemble those of a *bni1* single mutant and differ from those of a *gic1 gic2* double mutant. Indeed, although *gic1/gic1 gic2/gic2* double-mutant diploid cells appear to have a normal ellipsoidal cell shape (Figure 10, A and D), both *msb3/msb3 msb4/msb4* diploids (Figure 10B) and *bni1/bni1* diploids (Figure 10C) display cells that are rounder than normal. In addition, mutation of *MSB3* and *MSB4* and mutation of *BNI1* have similar effects on budding pattern. It has been shown previously that deletion of *BNI1* has little or no effect on the axial budding of haploid cells but that a diploid homozygous for the *bni1* deletion has a random budding pattern in which even the first bud on a daughter cell appears randomly positioned (Zahner *et al.*, 1996; Imamura *et al.*, 1997; Figure 10C). Similarly, *msb3, msb4,* and *msb3 msb4* haploids displayed normal axial budding (our unpublished results), but an *msb3/msb3 msb4/msb4* diploid displayed a random budding pattern (Figure 10B). (Diploid strains homozygous for deletions of *MSB3* alone or of *MSB4* alone displayed normal bipolar budding [our unpublished results].) Like the *bni1/bni1* strains (but unlike several other mutants with defects in bipolar budding; Zahner *et al.*, 1996; Yang *et al.*, 1997), the *msb3/msb3 msb4/msb4* strain frequently mispositioned even the first buds on daughter cells (our unpublished results). In contrast, deletion of *GIC1, GIC2,* or both had no obvious effect on the budding patterns of either haploid (our unpublished results) or diploid (Figure 10D) strains in the genetic background used here. Finally, examination of the Calcofluor-stained cells also revealed that both *bni1/bni1* cells and *msb3/msb3 msb4/msb4* cells, but not *gic1/gic1 gic2/gic2* cells, produced bud scars that were heterogeneous in size (Figure 10, B–D).

Why might the cell have two parallel pathways linking Cdc42p to the actin cytoskeleton? A clue comes from the observation that the *msb3 msb4* double-mutant haploids and the *msb3/msb3 msb4/msb4* double-mutant diploids have more severe growth and morphological defects at 23°C than at 37°C (Figures 5A, sector 4, and 10E, sectors 2 and 6; our unpublished results). Moreover, the morphological abnormalities observed at 23°C were more pronounced in the double-mutant diploid than in the double-mutant haploid (Figure 10, F and G). Similarly, deletion of *BNI1* causes more severe growth and morphological defects in a homozygous diploid than in a haploid and at low than at high temperatures (Figure 10E, sectors 3 and 7; Fares and Pringle, unpublished results). In striking contrast, a *gic1 gic2* double-mutant haploid is viable at 23°C but not at temperatures above 32°C (Brown *et al.*, 1997; Chen *et al.*, 1997a; Figures 9A and 10E, sector 4), whereas a *gic1/gic1 gic2/gic2* double-mutant diploid grew well even at 37°C (Figure 10E, sector 8). (In a different genetic background, a *gic1/gic1 gic2/gic2* double-mutant diploid grew at 35°C but not at 37°C [Chen and Chan, unpublished data].) Thus, it appears that the two pathways may differ in importance in different cell types and at different growth temperatures.

Evidence for a Cdc24p Function Distinct from Its Cdc42p-GEF Activity

All *cdc24*^{ts} alleles that have been examined are suppressed by multicopy *CDC42*, either alone or in combination with multicopy *MSB1, CLA4*, MSB3,* or *MSB4,* genes whose products all appear to be involved in the Cdc24p–Cdc42p pathway. These observations suggest that the available *cdc24*^{ts} alleles all encode products that are defective in the

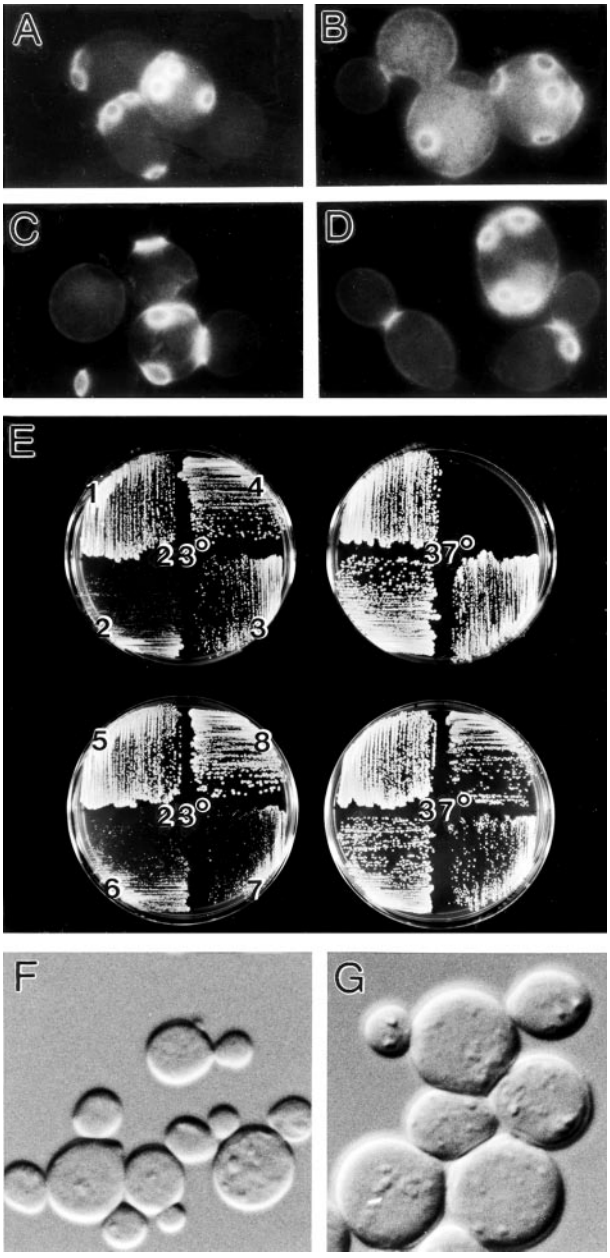

Figure 10. Comparison of *msb3 msb4, bni1,* and *gic1 gic2* mutant phenotypes. (A–D) Cells of diploid wild-type strain YEF473 (A), *msb3*Δ*::HIS3/msb3*Δ*::HIS3 msb4*Δ*::TRP1/msb4*Δ*::TRP1* strain YEF1631 (B), *bni1*Δ*::HIS3/bni1*Δ*::HIS3* strain HH799 (C), and *gic1*-Δ*1::LEU2/gic1*-Δ*1::LEU2 gic2*-Δ*2::TRP1/gic2*-Δ*2::TRP1* strain YEF1662 (D) were grown to exponential phase in YM-P liquid medium at 23°C, then fixed and stained with Calcofluor. (E) Haploid wild-type strain YEF473A (1), *msb3*Δ*::HIS3 msb4*Δ*::HIS3* strain YEF1269 (2), *bni1*Δ*::HIS3* strain YJZ426 (3), *gic1*-Δ*1::LEU2 gic2*-Δ*2::TRP1* strain CCY1042–12B (4), and diploid strains YEF473 (5), YEF1631 (6), HH799 (7), and YEF1662 (8) were streaked onto YPD plates and incubated for 2 days at the indicated temperatures. (F and G) Cells of *msb3 msb4* double-mutant haploid strain YEF1269 (F) and of double-mutant diploid strain YEF1631 (G) were grown to exponential phase in YM-P liquid medium at 23°C and examined by DIC microscopy. A–D, F, and G are printed at the same magnification.

interaction with Cdc42p and/or in the GEF activity. If Cdc24p really functions only as a Cdc42p GEF, then cells lacking Cdc24p might survive if the level of Cdc42p GAP activity is reduced. To test this possibility, we generated a *TRP1*-marked *cdc24* deletion in a diploid homozygous for deletions of both *BEM3* and *RGA1,* yielding strain YEF1265 (Table 1). Tetrad analysis of this strain yielded only Trp^- viable segregants. Thus, deletion of the two Cdc42p GAP genes cannot bypass the requirement for Cdc24p.

In a second experiment, we asked whether overexpression of other proteins involved in Cdc42p function would allow polarity establishment in the absence of Cdc24p. To this end, strain YEF1201, a *cdc24* deletion strain harboring a low-copy *GAL1-CDC24* plasmid, was transformed with high-copy plasmids containing *CDC42* alone or *CDC42* in combination with *CLA4*, MSB1*, or both. During growth of the resulting strains under mildly inducing conditions, Cdc24p levels were slightly greater than in wild-type cells (Figure 11A, lanes 1–4 and 9). After shift to repressing conditions for 16 h, Cdc24p was essentially undetectable in all strains (Figure 11A, lanes 5–8), indicating that overexpression of the other proteins had not stabilized Cdc24p. The presence of high-copy *CDC42* alone did not prevent Cdc24p-depleted cells from losing actin polarization and arresting uniformly as large, round cells (Figure 11, B and F). However, high-copy *CDC42* together with high-copy *CLA4** (Figure 11, C and G), high-copy *MSB1* (Figure 11, D and H), or both (Figure 11, E and I) allowed Cdc24p-depleted cells to polarize their actin cytoskeletons and cell growth. Approximately 50% of the *CLA4**-containing cells became polarized and were able to produce one bud-like structure per mother cell, and nearly all of the *MSB1*-containing or *MSB1*- and *CLA4**-containing cells became polarized and were able to produce multiple (up to three or four) elongated bud-like structures per cell. However, none of the strains tested was able to form colonies under the repressing conditions for *CDC24* expression, suggesting that Cdc24p has at least one function in addition to activating polarity establishment through its Cdc42p GEF activity.

DISCUSSION

The Possibility of a Cdc24p Function Distinct from Its Cdc42p GEF Activity

Although it is well established that Cdc24p functions as an activating factor (GEF) for Cdc42p, it also seems possible that Cdc24p has one or more other targets (see INTRODUCTION). The genetic screens undertaken in this study were designed to seek such additional targets. However, as discussed below, all of the genes actually identified encode products that appear to function in the Cdc42p pathway. Nonetheless, we also obtained some evidence suggesting that Cdc24p might not function exclusively as a Cdc42p GEF. First, we observed that Cdc24p was still essential for growth in a strain in which the genes encoding the Cdc42p GAPs Bem3p and Rga1p (Zheng *et al.*, 1994b; Stevenson *et al.*, 1995) had been deleted. In contrast, in the *S. cerevisiae* Ras pathway, deletion of GAP-encoding genes rescues the inviability of mutants defective in the GEF Cdc25p (Tanaka *et al.*, 1989, 1990a, 1990b), suggesting that the GEF is required only to counteract the activity of the GAPs. However, this argument is weakened by the possibility that Cdc24p may be

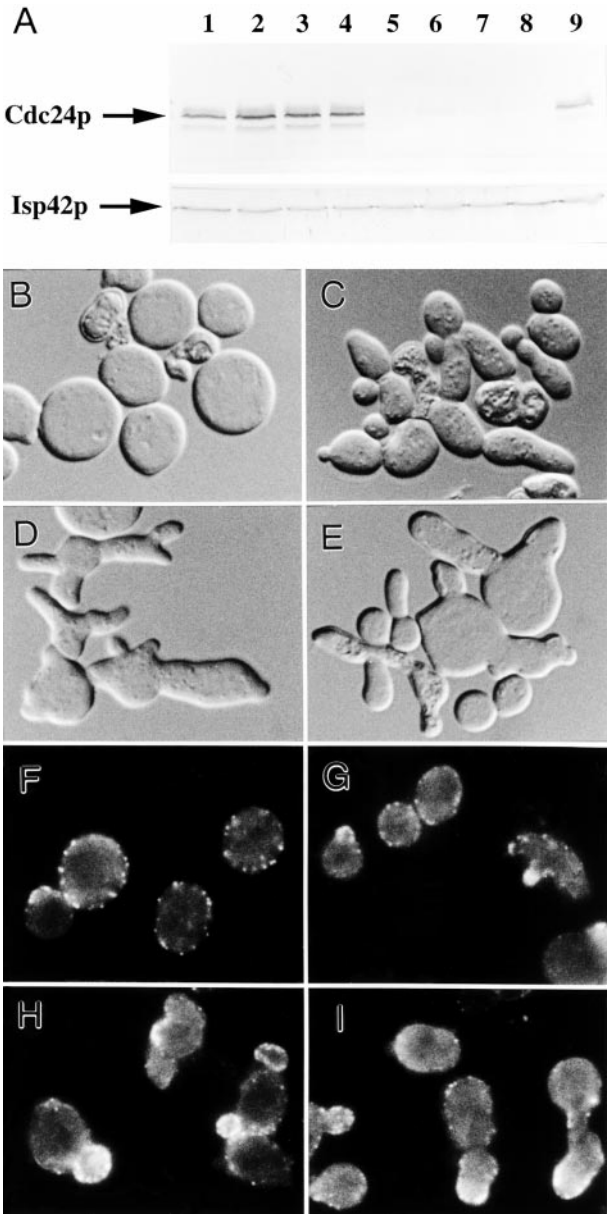

Figure 11. Polarity establishment in the absence of Cdc24p. (A) Western-blot analysis using antibodies to Cdc24p and (as a control) the mitochondrial outer membrane protein Isp42p. (B–E) Cell morphologies as observed by DIC microscopy. (F–I) Immunolocalization of actin using anti-actin antibodies. Strain YEF1201 (*cdc24Δ::HIS3* [pMGF5]) was transformed with plasmids YEp352-CDC42 and YEp13 (A, lanes 1 and 5, B, and F), YEp352-CDC42 and YEp13-CLA4* (A, lanes 2 and 6, C, and G), YEp352-CDC42 and YEp13-MSB1 (A, lanes 3 and 7, D, and H), or YEp352–42CLA4* and YEp13-MSB1 (A, lanes 4 and 8, E, I). Cells were grown to exponential phase at 30°C under mildly inducing conditions for *GAL1-CDC24* (SC-Leu-Ura liquid medium containing 2% glucose plus 2% galactose), and samples were removed for immunoblot analysis (A, lanes 1–4). Cells were then shifted to repressing conditions (SC-Leu-Ura liquid medium containing 2% glucose only) for 12 h, diluted further with the same medium, and incubated for an additional 4 h before harvesting for immunoblot (A, lanes 5–8) and microscopic (B–I) analysis. Wild-type strain YEF473 growing exponentially in liquid SC medium at 30°C was used as a control (A, lane 9). B–I are printed at the same magnification.

required to compensate for the relatively high intrinsic GTPase activity of Cdc42p (Zheng *et al.*, 1994b) and by the likelihood that there are Cdc42p GAPs in addition to Bem3p and Rga1p (Bi and Pringle, 1996; Chen *et al.*, 1997a; Bose and Lew, personal communication; Sprague, personal communication).

Thus, a more persuasive argument is provided by the observation that the presence of high-copy *CDC42* together with high-copy *CLA4**, high-copy *MSB1*, or both allowed Cdc24p-depleted cells to polarize their actin cytoskeletons and produce multiple bud-like structures, although they could not complete the cell cycle and divide. This phenotype might reflect rescue of the Cdc42p pathway, but not of another Cdc24p-dependent pathway, in these cells. However, until another Cdc24p target has actually been identified, its existence remains uncertain, and it is possible that the other domains of Cdc24p function solely in the temporal and spatial regulation of its interaction with Cdc42p. For example, the Ca^{2+}-binding sites may regulate the interaction between Cdc24p/Cdc42p and Bem1p (Zheng *et al.*, 1995), and the PH domain may serve to bind regulatory ligands or as a membrane adaptor for Cdc24p and its associated proteins (Hemmings, 1997; Aghazadeh *et al.*, 1998; Lemmon and Ferguson, 1998; Liu *et al.*, 1998; Rebecchi and Scarlata, 1998; Soisson *et al.*, 1998).

Interaction of Cla4p and Msb1p with Cdc24p and Cdc42p

Of the three genes identified in our screens, two were the previously known *CLA4* and *MSB1*. Overexpression of the truncated *CLA4** alone, of MSB1 alone, or of *CLA4** and *MSB1* together could suppress the *cdc24-11* mutation only when *CDC42* was also overexpressed. These observations might be taken to mean that the *cdc24-11* mutant is defective in each of two Cdc24p-controlled pathways, one of which involves Cdc42p and the other of which involves Cla4p and/or Msb1p. However, abundant other evidence indicates that both Cla4p and Msb1p actually function in conjunction with Cdc42p. In the case of Cla4p, we observed that multicopy *CLA4** by itself could suppress a *cdc42-1* mutation but not any of several *cdc24* alleles (Figure 1B). In addition, Cla4p is a member of the PAK kinase family, for which binding to and activation by the GTP-bound form of Cdc42p and its homologues are well established, although the targets of the activated PAKs themselves remain unclear (Cvrčková *et al.*, 1995; Simon *et al.*, 1995; Peter *et al.*, 1996; Benton *et al.*, 1997; Leberer *et al.*, 1997; Sells and Chernoff, 1997; Van Aelst and D'Souza-Schorey, 1997; Eby *et al.*, 1998; Hall, 1998; Johnson, 1999). Binding to PAK has been shown to inhibit the intrinsic GTPase activity of human Cdc42 (Manser *et al.*, 1994). This suggests that overexpression of Cla4p*, which lacks the Cla4p kinase domain but includes its Cdc42p-binding CRIB domain, suppresses *cdc42-1* or (when *CDC42* is also overexpressed) *cdc24-11* by inhibiting the intrinsic GTPase activity of Cdc42p and thus increasing the fraction of the protein that is in the active state. Interestingly, full-length *CLA4* lacked the suppressor activities of *CLA4**, suggesting that the binding of Cla4p to Cdc42p may be regulated by the kinase activity or by the presence of the kinase domain.

The evidence that Msb1p functions in conjunction with Cdc42p is less direct but nonetheless good. *MSB1* was first

identified as a multicopy suppressor of the *cdc24-4* mutation, which is also suppressed well by multicopy *CDC42,* and multicopy *MSB1* also suppresses *cdc42-1* at least as well as it suppresses *cdc24-4* (Bender and Pringle, 1989; Figure 1B). In addition, *MSB1* is a multicopy suppressor of mutations in *BEM4,* whose product appears to interact with Cdc42p (Mack *et al.*, 1996), and an *msb1* deletion is synthetically lethal with mutations in *BEM2* (Bender and Pringle, 1991), whose product may also interact with Cdc42p (Chen *et al.*, 1996, 1997a). Finally, Msb1p colocalizes with Cdc42p throughout the cell cycle (Bi and Pringle, unpublished results). Msb1p is a protein of 1137 amino acids for which biochemical activities or close homologies have not yet been found; it may function as a scaffold that helps assemble Cdc24p, Cdc42p, and other proteins into a functional complex. Thus, overexpression of Msb1p might suppress *cdc24* and *cdc42* mutations by promoting the more efficient assembly or function of such complexes or by directing them to appropriate intracellular locations.

Parallel Pathways Linking Cdc42p to Actin Polarization

The third gene identified in our screen was the novel *MSB3.* The genome sequence revealed that *MSB3* has a close structural homologue, *MSB4,* and several lines of evidence indicate that Msb3p and Msb4p have overlapping functions in a pathway that links the activation of Cdc42p to polarization of the cytoskeleton. First, Msb3p and Msb4p colocalized with each other and with Cdc42p to a patch at the presumptive bud site, to the tip of the growing bud, and (just before division) to the mother-bud neck. (Localization of Cdc42p to the neck was not consistently visualized with anti-Cdc42p antibodies [Ziman *et al.*, 1993] but is apparent using HA- or GFP-tagged Cdc42p [Johnson, 1999; Bi and Pringle, unpublished results].) Moreover, the localization of Msb3p and Msb4p depended on the function of Cdc42p (Figure 8, D–I), whereas Cdc42p localized normally in an *msb3 msb4* strain (Bi and Pringle, unpublished results). Second, overexpression of either *MSB3* or *MSB4* suppressed *cdc24-11* efficiently when *CDC42* was also overexpressed, but each gene suppressed *cdc24* alleles weakly or not at all in the absence of *CDC42* overexpression. In contrast, overexpression of *MSB3* by itself suppressed *cdc42-1* efficiently. (The failure to observe suppression of *cdc42* by multicopy *MSB4* may reflect the fact that only one *cdc42*^{ts} allele was available for testing.) Third, although deletion of either *MSB3* or *MSB4* alone produced no obvious phenotype, the *msb3 msb4* double mutant displayed a partial loss of cell polarization resembling that resulting from a loss of Cdc42p function. Moreover, deletion of both *MSB3* and *MSB4,* but not deletion of either gene alone, was lethal in a *gic1 gic2* background (also see below). Finally, the phenotype of the *msb3 msb4* double mutant closely resembled that resulting from deletion of *BNI1,* a gene whose product appears to function downstream of Cdc42p (and perhaps Rho1p) in a pathway(s) leading to cytoskeletal polarization (Evangelista *et al.*, 1997; Frazier and Field, 1997; Imamura *et al.*, 1997; Fujiwara *et al.*, 1998; Umikawa *et al.*, 1998; Wasserman, 1998).

Cdc42p is necessary for polarization both of the actin cytoskeleton and of the septins (Adams and Pringle, 1984; Adams *et al.*, 1990; Li *et al.*, 1995; Pringle *et al.*, 1995), but polarization of actin and of the septins are independent of each other (Adams and Pringle, 1984; Ford and Pringle, 1991; Ayscough *et al.*, 1997). Two lines of evidence suggest strongly that Msb3p and Msb4p are involved specifically in a pathway leading to actin polarization. First, the localization of Msb3p and Msb4p through the cell cycle (see above) resembles the localization of actin and associated proteins (Botstein *et al.*, 1997; Bi *et al.*, 1998; Lippincott and Li, 1998) more closely than it does that of the septins, which form a ring at the presumptive bud site and remain at the mother-bud neck throughout the cell cycle (Longtine *et al.*, 1996). Second, and more convincing, the large, round cells in an *msb3 msb4* double-mutant strain displayed relatively normal septin rings despite their loss of actin polarization (Figure 6, D–F).

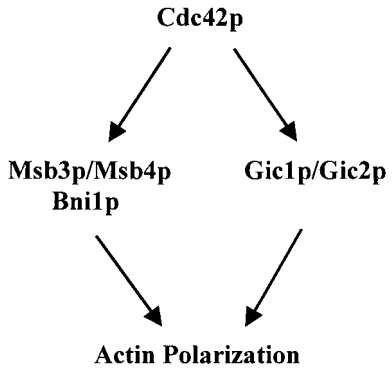

Figure 12. Parallel pathways for signaling from Cdc42p to the actin cytoskeleton. See text for details.

If the Msb3p/Msb4p pathway is important for actin polarization, why do *msb3 msb4* double-mutant cells survive? It appears that this is because the Msb3p/Msb4p pathway is largely redundant in function with a distinct pathway involving Gic1p and Gic2p (Figure 12). Multiple lines of evidence indicate that Gic1p and Gic2p function redundantly with each other in a pathway that is important, but not essential, for the Cdc42p-mediated polarization of the actin cytoskeleton (Brown *et al.*, 1997; Chen *et al.*, 1997a; Jaquenoud *et al.*, 1998; Richman *et al.*, 1999). The viability of the *gic1 gic2* double mutant and the observation that its phenotypes could be suppressed by overexpression of *CDC42* (Brown *et al.*, 1997; Chen *et al.*, 1997a) had already suggested the existence of a redundant pathway, and we have shown here that overexpression of *MSB3* or *MSB4* can also partially suppress the *gic1 gic2* double mutant. Moreover, although all double and triple mutants involving *msb3, msb4, gic1,* and *gic2* deletions were viable, the quadruple mutant was inviable and displayed a loss-of-polarity phenotype.

A variety of other proteins have also been implicated in the communication between Cdc42p and the actin cytoskeleton (see INTRODUCTION), and it is important to determine how the functions of these other proteins relate to the pathways defined by Msb3p/Msb4p and by Gic1p/Gic2p. To date, the only clear evidence is for Bni1p, for which several observations indicate a role in the pathway involving Msb3p and Msb4p. First, the *bni1* single mutant and the *msb3 msb4* double mutant have similarities in the details of their phenotypes that are not shared with the *gic1 gic2* double mutant (see RESULTS). These distinctions may re-

flect aspects of Msb3p/Msb4p/Bni1p pathway function that are not fully redundant with the Gic1p/Gic2p pathway, which may in turn explain why we observed no suppression of the *msb3 msb4* phenotypes by overexpression of Gic1p or Gic2p (in contrast to the suppression of *gic1 gic2* phenotypes by overexpression of Msb3p or Msb4p). Second, *msb3 msb4 bni1* triple mutants were viable, whereas the *bni1 gic1 gic2* triple mutants, like the *msb3 msb4 gic1 gic2* quadruple mutants, were inviable. It is not yet clear whether Bni1p should be viewed as functioning upstream or downstream of Msb3p and Msb4p. Indeed, given the evidence that Bni1p interacts directly both with Cdc42p GTP and with components of the actin cytoskeleton (Kohno *et al.*, 1996; Evangelista *et al.*, 1997; Frazier and Field, 1997; Imamura *et al.*, 1997; Fujiwara *et al.*, 1998; Umikawa *et al.*, 1998; Wasserman, 1998), it seems more likely that the question is meaningless because the proteins actually all function as part of a single complex. However, the specific binding interactions of Msb3p and Msb4p have not yet been defined. In particular, these proteins do not contain recognizable Cdc42p-interaction domains, and there is as yet no evidence for a direct interaction between them and Cdc42p, Bni1p, or components of the actin cytoskeleton.

The evidence that the Msb3p/Msb4p/Bni1p pathway and the Gic1p/Gic2p pathway are largely redundant in function raises the now-common question of why such redundancy has evolved. In the present case, the data suggest that the two parallel pathways may be optimized for the physiological states obtaining in different cell types and under different growth conditions. In particular, it appears that the Msb3p/Msb4p/Bni1p pathway is more important in diploids and at lower growth temperatures, whereas the Gic1p/Gic2p pathway is more important in haploids and at higher growth temperatures, and it seems likely that other variations in growth conditions would reveal other illustrations of the differential importance of the two pathways.

Possible Evolutionary Conservation of Msb3p/Msb4p Function

Both the structure of Cdc42p and its role in organizing the actin cytoskeleton have been strongly conserved during eukaryotic evolution (see INTRODUCTION). This conservation extends also to many of the apparent regulators and effectors of Cdc42p (see INTRODUCTION). In particular, proteins with similar sequence organization and significant sequence homology to Bni1p (the FH proteins) appear to be involved in linking Rho-type GTPases to the actin cytoskeleton in other fungi, nematodes, flies, and mammals, as well as in yeast (Frazier and Field, 1997; Wasserman, 1998). In this context, it seems likely that the role of Msb3p/Msb4p-type proteins in a pathway involving also an FH protein would also have been conserved. However, the available data do not allow a clear conclusion on this point. Msb3p and Msb4p are indeed members of a large protein family (see RESULTS and Figure 3). However, among the known family members, only *S. pombe* SpMsb3p has strong homology with Msb3p and Msb4p over the full lengths of the proteins, and the functions of SpMsb3p have not yet been investigated. In contrast, the family members from multicellular organisms, such as Pollux and tre17, like the *S. cerevisiae* proteins Mdr1p and Ypl249Cp, share more limited homology with Msb3p and Msb4p over only a portion of the proteins, so that the sequence similarity provides no strong indicator of homologous function. Indeed, for Mdr1p and Ypl249Cp, gene deletions produced no obvious phenotype and did not obviously enhance the phenotype caused by deletion of *MSB3* and *MSB4,* suggesting that Mdr1p and Ypl249Cp function in another pathway(s). The available information about the proteins from multicellular organisms is also not very helpful at this time. Pollux has been reported to be both a possible cell-adhesion molecule (Zhang *et al.*, 1996) and a calmodulin-binding protein (Xu *et al.*, 1998), both properties that could be associated with a role in cytoskeletal organization, but its actual function remains obscure. *tre17* has been identified as an oncogene by several criteria (Nakamura *et al.*, 1992; Onno *et al.*, 1993), but there appear to be no good clues to the origins of its oncogenicity. Nonetheless, it is intriguing that a loss of normal cell shape and polarization is a general property of cancer cells, so that a possible role for tre17 in morphogenesis is not implausible. Clearly, however, elucidation of the roles of these family members and of their shared and distinct functional domains will require further investigation.

Note Added in Proof. A recent paper by Albert and Gallwitz (J. Biol. Chem. *274*, 33186–33189, 1999) showed that Msb3p can function as a GAP for several Rab proteins including Sec4p. This suggests that Cdc42p-mediated actin organization may be coupled to a late secretion function through Msb3p and Msb4p.

ACKNOWLEDGMENTS

We thank Johnny Fares, Mark Longtine, and other past and present members of the Pringle laboratory for valuable discussions and encouragement; Emily Walsh for assistance with some experiments; Doug DeMarini for the genomic library; Alan Bender, Doug Johnson, Fatima Cvrčková, Kim Nasmyth, and Yoshi Ohya for plasmids; and John Cooper and Mike Douglas for antibodies. This work was supported by National Institutes of Health grants GM-31006 (to J.R.P.) and GM-45185 (to C.S.M.C.); by funds from the RJEG Trust (to J.R.P.) and the Texas Higher Education Coordinating Board (grant ARP-427 to C.S.M.C.); and by the Cancer Research Fund of the Damon Runyon–Walter Winchell Foundation (fellowship DRG-1197 to E.B.).

REFERENCES

Adams, A.E.M., Johnson, D.I., Longnecker, R.M., Sloat, B.F., and Pringle, J.R. (1990). *CDC42* and *CDC43*, two additional genes involved in budding and the establishment of cell polarity in the yeast *Saccharomyces cerevisiae*. J. Cell Biol. *111*, 131–142.

Adams, A.E.M., and Pringle, J.R. (1984). Relationship of actin and tubulin distribution to bud growth in wild-type and morphogenetic-mutant *Saccharomyces cerevisiae*. J. Cell Biol. *98*, 934–945.

Adams, A.E.M., and Pringle, J.R. (1991). Staining of actin with fluorochrome-conjugated phalloidin. Methods Enzymol. *194*, 729–731.

Aghazadeh, B., Zhu, K., Kubiseski, T.J., Liu, G.A., Pawson, T., Zheng, Y., and Rosen, M.K. (1998). Structure and mutagenesis of the Dbl homology domain. Nat. Struct. Biol. *5*, 1098–1107.

Amatruda, J.F., and Cooper, J.A. (1992). Purification, characterization, and immunofluorescence localization of *Saccharomyces cerevisiae* capping protein. J. Cell Biol. *117*, 1067–1076.

Aspenström, P. (1999). Effectors for the Rho GTPases. Curr. Opin. Cell Biol. *11*, 95–102.

Ayscough, K.R., Stryker, J., Pokala, N., Sanders, M., Crews, P., and Drubin, D.G. (1997). High rates of actin filament turnover in budding yeast and roles for actin in establishment and maintenance of cell polarity revealed using the actin inhibitor latrunculin-A. J. Cell Biol. *137*, 399–416.

Baudin, A., Ozier-Kalogeropoulos, O., Denouel, A., Lacroute, F., and Cullin, C. (1993). A simple and efficient method for direct gene deletion in *Saccharomyces cerevisiae*. Nucleic Acids Res. *21*, 3329–3330.

Bender, A., and Pringle, J.R. (1989). Multicopy suppression of the *cdc24* budding defect in yeast by *CDC42* and three newly identified genes including the *ras*-related gene. RSR1. Proc. Natl. Acad. Sci. USA *86*, 9976–9980.

Bender, A., and Pringle, J.R. (1991). Use of a screen for synthetic lethal and multicopy suppressee mutants to identify two new genes involved in morphogenesis in *Saccharomyces cerevisiae*. Mol. Cell. Biol. *11*, 1295–1305.

Bender, A., and Pringle, J.R. (1995). Cdc24p. In: Guidebook to the Small GTPases, ed. M. Zerial and L.A. Huber, Oxford: Oxford University Press, 288–291.

Benton, B.K., Tinkelenberg, A., Gonzalez, I., and Cross, F.R. (1997). Cla4p, a *Saccharomyces cerevisiae* Cdc42p-activated kinase involved in cytokinesis, is activated at mitosis. Mol. Cell. Biol. *17*, 5067–5076.

Bi, E., Maddox, P., Lew, D.J., Salmon, E.D., McMillan, J.N., Yeh, E., and Pringle, J.R. (1998). Involvement of an actomyosin contractile ring in *Saccharomyces cerevisiae* cytokinesis. J. Cell Biol. *142*, 1301–1312.

Bi, E., and Pringle, J.R. (1996). *ZDS1* and *ZDS2*, genes whose products may regulate Cdc42p in *Saccharomyces cerevisiae*. Mol. Cell. Biol. *16*, 5264–5275.

Bi, E., and Zigmond, S.H. (1999). Actin polymerization: where the WASP stings. Curr. Biol. *9*, R160–R163.

Botstein, D., Amberg, D., Mulholland, J., Huffaker, T., Adams, A., Drubin, D., and Stearns, T. (1997). The yeast cytoskeleton. In: The Molecular and Cellular Biology of the Yeast *Saccharomyces*, Cell Cycle and Cell Biology, ed. J.R. Pringle, J.R. Broach, and E.W. Jones, Cold Spring Harbor, NY: Cold Spring Harbor Laboratory Press, 1–90.

Brown, J.L., Jaquenoud, M., Gulli, M.-P., Chant, J., and Peter, M. (1997). Novel Cdc42-binding proteins Gic1 and Gic2 control cell polarity in yeast. Genes Dev. *11*, 2972–2982.

Burbelo, P.D., Drechsel, D., and Hall, A. (1995). A conserved binding motif defines numerous candidate target proteins for both Cdc42 and Rac GTPases. J. Biol. Chem. *270*, 29071–29074.

Cerione, R.A., and Zheng, Y. (1996). The Dbl family of oncogenes. Curr. Opin. Cell Biol. *8*, 216–222.

Chen, G.-C., Zheng, L., and Chan, C.S.M. (1996). The LIM domain-containing Dbm1 GTPase-activating protein is required for normal cellular morphogenesis in *Saccharomyces cerevisiae*. Mol. Cell. Biol. *16*, 1376–1390.

Chen, G.-C., Kim, Y.-J., and Chan, C.S.M. (1997a). The Cdc42 GTPase-associated proteins Gic1 and Gic2 are required for polarized cell growth in *Saccharomyces cerevisiae*. Genes Dev. *11*, 2958–2971.

Chen, P., Sapperstein, S.K., Choi, J.D., and Michaelis, S. (1997b). Biogenesis of the *Saccharomyces cerevisiae* mating pheromone a-factor. J. Cell Biol. *136*, 251–269.

Cid, V.J., Durán, A., del Rey, F., Snyder, M.P., Nombela, C., and Sánchez, M. (1995). Molecular basis of cell integrity and morphogenesis in *Saccharomyces cerevisiae*. Microbiol. Rev. *59*, 345–386.

Cvrčková, F., De Virgilio, C., Manser, E., Pringle, J.R., and Nasmyth, K. (1995). Ste20-like protein kinases are required for normal localization of cell growth and for cytokinesis in budding yeast. Genes Dev. *9*, 1817–1830.

DeMarini, D.J., Adams, A.E.M., Fares, H., De Virgilio, C., Valle, G., Chuang, J.S., and Pringle, J.R. (1997). A septin-based hierarchy of proteins required for localized deposition of chitin in the *Saccharomyces cerevisiae* cell wall. J. Cell Biol. *139*, 75–93.

De Virgilio, C., DeMarini, D.J., and Pringle, J.R. (1996). *SPR28*, a sixth member of the septin gene family in *Saccharomyces cerevisiae* that is expressed specifically in sporulating cells. Microbiology *142*, 2897–2905.

Drubin, D.G., and Nelson, W.J. (1996). Origins of cell polarity. Cell *84*, 335–344.

Eby, J.J., Holly, S.P., van Drogen, F., Grishin, A.V., Peter, M., Drubin, D.G., and Blumer, K.J. (1998). Actin cytoskeletal organization regulated by the PAK family of protein kinases. Curr. Biol. *8*, 967–970.

Epp, J.A., and Chant, J. (1997). An IQGAP-related protein controls actin-ring formation and cytokinesis in yeast. Curr. Biol. *7*, 921–929.

Evangelista, M., Blundell, K., Longtine, M.S., Chow, C.J., Adames, N., Pringle, J.R., Peter, M., and Boone, C. (1997). Bni1p, a yeast formin linking Cdc42p and the actin cytoskeleton during polarized morphogenesis. Science *276*, 118–122.

Ford, S.K., and Pringle, J.R. (1991). Cellular morphogenesis in the *Saccharomyces cerevisiae* cell cycle: localization of the *CDC11* gene product and the timing of events at the budding site. Dev. Genet. *12*, 281–292.

Frazier, J.A., and Field, C.M. (1997). Actin cytoskeleton: are FH proteins local organizers? Curr. Biol. *7*, R414–R417.

Fujiwara, T., Tanaka, K., Mino, A., Kikyo, M., Takahashi, K., Shimizu, K., and Takai, Y. (1998). Rho1p-Bni1p-Spa2p interactions: implication in localization of Bni1p at the bud site and regulation of the actin cytoskeleton in *Saccharomyces cerevisiae*. Mol. Biol. Cell *9*, 1221–1233.

Gietz, R.D., and Sugino, A. (1988). New yeast-*Escherichia coli* shuttle vectors constructed with in vitro mutagenized yeast genes lacking six-base pair restriction sites. Gene *74*, 527–534.

Guthrie, C., and Fink, G.R., ed. (1991). Guide to Yeast Genetics and Molecular Biology. Methods Enzymol., vol. *194*, San Diego: Academic Press.

Hall, A. (1998). Rho GTPases and the actin cytoskeleton. Science *279*, 509–514.

Harris, S.D., and Pringle, J.R. (1991). Genetic analysis of *Saccharomyces cerevisiae* chromosome I: on the role of mutagen specificity in delimiting the set of genes identifiable using temperature-sensitive-lethal mutations. Genetics *127*, 279–285.

Hart, M.J., Eva, A., Zangrilli, D., Aaronson, S.A., Evans, T., Cerione, R.A., and Zheng, Y. (1994). Cellular transformation and guanine nucleotide exchange activity are catalyzed by a common domain on the *dbl* oncogene product. J. Biol. Chem. *269*, 62–65.

Hartwell, L.H., Culotti, J., Pringle, J.R., and Reid, B.J. (1974). Genetic control of the cell division cycle in yeast. Science *183*, 46–51.

Hemmings, B.A. (1997). PH domains—a universal membrane adaptor. Science *275*, 1899.

Hill, J.E., Myers, A.M., Koerner, T.J., and Tzagoloff, A. (1986). Yeast/*E. coli* shuttle vectors with multiple unique restriction sites. Yeast *2*, 163–167.

Hofmann, K., and Stoffel, W. (1993). A database of membrane spanning protein segments. Biol. Chem. Hoppe-Seyler *374*, 166.

Horii, Y., Beeler, J.F., Sakaguchi, K., Tachibana, M., and Miki, T. (1994). A novel oncogene, *ost*, encodes a guanine nucleotide exchange factor that potentially links Rho and Rac signaling pathways. EMBO J. *13*, 4776–4786.

Imamura, H., Tanaka, K., Hihara, T., Umikawa, M., Kamei, T., Takahashi, K., Sasaki, T., and Takai, Y. (1997). Bni1p and Bnr1p: downstream targets of the Rho family small G-proteins which interact with profilin and regulate actin cytoskeleton in *Saccharomyces cerevisiae*. EMBO J. *16,* 2745–2755.

Jansen, R.-P., Dowzer, C., Michaelis, C., Galova, M., and Nasmyth, K. (1996). Mother cell-specific *HO* expression in budding yeast depends on the unconventional myosin Myo4p and other cytoplasmic proteins. Cell *84*, 687–697.

Jaquenoud, M., Gulli, M.-P., Peter, K., and Peter, M. (1998). The Cdc42p effector Gic2p is targeted for ubiquitin-dependent degradation by the SCF^{Grr1} complex. EMBO J. *17,* 5360–5373.

Johnson, D.I. (1999). Cdc42: an essential Rho-type GTPase controlling eukaryotic cell polarity. Microbiol. Mol. Biol. Rev. *63*, 54–105.

Johnson, D.I., and Pringle, J.R. (1990). Molecular characterization of *CDC42*, a *Saccharomyces cerevisiae* gene involved in the development of cell polarity. J. Cell Biol. *111*, 143–152.

Karpova, T.S., Lepetit, M.M., and Cooper, J.A. (1993). Mutations that enhance the *cap2* null mutant phenotype in *Saccharomyces cerevisiae* affect the actin cytoskeleton, morphogenesis and pattern of growth. Genetics *135,* 693–709.

Kassenbrock, C.K., Cao, W., and Douglas, M.G. (1993). Genetic and biochemical characterization of ISP6, a small mitochondrial outer membrane protein associated with the protein translocation complex. EMBO J. *12*, 3023–3034.

Kilmartin, J.V., and Adams, A.E.M. (1984). Structural rearrangements of tubulin and actin during the cell cycle of the yeast *Saccharomyces cerevisiae*. J. Cell Biol. *98*, 922–933.

Kilmartin, J.V., Wright, B., and Milstein, C. (1982). Rat monoclonal antitubulin antibodies derived by using a new nonsecreting rat cell line. J. Cell Biol. *93*, 576–582.

Koch, G., Tanaka, K., Masuda, T., Yamochi, W., Nonaka, H., and Takai, Y. (1997). Association of the Rho family small GTP-binding proteins with Rho GDP dissociation inhibitor (Rho GDI) in *Saccharomyces cerevisiae.* Oncogene *15,* 417–422.

Kohno, H., *et al*. (1996). Bni1p implicated in cytoskeletal control is a putative target of Rho1p small GTP-binding protein in *Saccharomyces cerevisiae.* EMBO J. *15,* 6060–6068.

Laemmli, U.K. (1970). Cleavage of structural proteins during the assembly of the head of bacteriophage T4. Nature *227*, 680–685.

Lamarche, N., and Hall, A. (1994). GAPs for rho-related GTPases. Trends Genet. *10*, 436–440.

Leberer, E., Wu, C., Leeuw, T., Fourest-Lieuvin, A., Segall, J.E., and Thomas, D.Y. (1997). Functional characterization of the Cdc42p binding domain of yeast Ste20p protein kinase. EMBO J. *16*, 83–97.

Lemmon, M.A., and Ferguson, K.M. (1998). Pleckstrin homology domains. Curr. Top. Microbiol. Immunol. *228*, 39–74.

Lew, D.J., and Reed, S.I. (1993). Morphogenesis in the yeast cell cycle: regulation by Cdc28 and cyclins. J. Cell Biol. *120*, 1305–1320.

Li, R. (1997). Bee1, a yeast protein with homology to Wiscott-Aldrich Syndrome Protein, is critical for the assembly of cortical actin cytoskeleton. J. Cell Biol. *136*, 649–658.

Li, R., Zheng, Y., and Drubin, D.G. (1995). Regulation of cortical actin cytoskeleton assembly during polarized cell growth in budding yeast. J. Cell Biol. *128*, 599–615.

Lillie, S.H., and Pringle, J.R. (1980). Reserve carbohydrate metabolism in *Saccharomyces cerevisiae*: responses to nutrient limitation. J. Bacteriol. *143,* 1384–1394.

Lippincott, J., and Li, R. (1998). Sequential assembly of myosin II, an IQGAP-like protein, and filamentous actin to a ring structure involved in budding yeast cytokinesis. J. Cell Biol. *140*, 355–366.

Liu, X., *et al*. (1998). NMR structure and mutagenesis of the N-terminal Dbl homology domain of the nucleotide exchange factor Trio. Cell *95*, 269–277.

Longtine, M.S., DeMarini, D.J., Valencik, M.L., Al-Awar, O.S., Fares, H., De Virgilio, C., and Pringle, J.R. (1996). The septins: roles in cytokinesis and other processes. Curr. Opin. Cell Biol. *8*, 106–119.

Lupas, A. (1996). Prediction and analysis of coiled-coil structures. Methods Enzymol. *266*, 513–525.

Machesky, L.M. (1998). Cytokinesis: IQGAPs find a function. Curr. Biol. *8*, R202–R205.

Mack, D., Nishimura, K., Dennehey, B.K., Arbogast, T., Parkinson, J., Toh-e, A., Pringle, J.R., Bender, A., and Matsui, Y. (1996). Identification of the bud emergence gene *BEM4* and its interactions with Rho-type GTPases in *Saccharomyces cerevisiae.* Mol. Cell. Biol. *16,* 4387–4395.

Manser, E., Leung, T., Salihuddin, H., Zhao, Z., and Lim, L. (1994). A brain serine/threonine protein kinase activated by Cdc42 and Rac1. Nature *367*, 40–46.

Martín, H., Mendoza, A., Rodríguez-Pachón, J.M., Molina, M., and Nombela, C. (1997). Characterization of *SKM1*, a *Saccharomyces cerevisiae* gene encoding a novel Ste20/PAK-like protein kinase. Mol. Microbiol. *23*, 431–444.

Miyamoto, S., Ohya, Y., Sano, Y., Sakaguchi, S., Iida, H., and Anraku, Y. (1991). A *DBL*-homologous region of the yeast *CLS4*/*CDC24* gene product is important for Ca^{2+}-modulated bud assembly. Biochem. Biophys. Res. Commun. *181*, 604–610.

Nakamura, T., Hillova, J., Mariage-Samson, R., Onno, M., Huebner, K., Cannizzaro, L.A., Boghosian-Sell, L., Croce, C.M., and Hill, M. (1992). A novel transcriptional unit of the *tre* oncogene widely expressed in human cancer cells. Oncogene *7*, 733–741.

Naqvi, S.N., Zahn, R., Mitchell, D.A., Stevenson, B.J., and Munn, A.L. (1998). The WASp homologue Las17p functions with the WIP homologue End5p/verprolin and is essential for endocytosis in yeast. Curr. Biol. *8*, 959–962.

Ohya, Y., Miyamoto, S., Ohsumi, Y., and Anraku, Y. (1986). Calcium-sensitive *cls4* mutant of *Saccharomyces cerevisiae* with a defect in bud formation. J. Bacteriol. *165*, 28–33.

Onno, M., Nakamura, T., Mariage-Samson, R., Hillova, J., and Hill, M. (1993). Human TRE17 oncogene is generated from a family of homologous polymorphic sequences by single-base changes. DNA Cell Biol. *12*, 107–118.

Osman, M.A., and Cerione, R.A. (1998). Iqg1p, a yeast homologue of the mammalian IQGAPs, mediates Cdc42p effects on the actin cytoskeleton. J. Cell Biol. *142*, 443–455.

Park, H.-O., Bi, E., Pringle, J.R., and Herskowitz, I. (1997). Two active states of the Ras-related Bud1/Rsr1 protein bind to different effectors to determine yeast cell polarity. Proc. Natl. Acad. Sci. USA *94*, 4463–4468.

Peter, M., Neiman, A.M., Park, H.-O., van Lohuizen, M., and Herskowitz, I. (1996). Functional analysis of the interaction between the small GTP binding protein Cdc42 and the Ste20 protein kinase in yeast. EMBO J. *15*, 7046–7059.

Peterson, J., Zheng, Y., Bender, L., Myers, A., Cerione, R., and Bender, A. (1994). Interactions between the bud emergence proteins Bem1p and Bem2p and Rho-type GTPases in yeast. J. Cell Biol. *127*, 1395–1406.

Pringle, J.R. (1991). Staining of bud scars and other cell wall chitin with Calcofluor. Methods Enzymol. *194*, 732–735.

Pringle, J.R., Adams, A.E.M., Drubin, D.G., and Haarer, B.K. (1991). Immunofluorescence methods for yeast. Methods Enzymol. *194*, 565–602.

Pringle, J.R., Bi, E., Harkins, H.A., Zahner, J.E., De Virgilio, C., Chant, J., Corrado, K., and Fares, H. (1995). Establishment of cell polarity in yeast. Cold Spring Harbor Symp. Quant. Biol. *60*, 729–743.

Pringle, J.R., and Hartwell, L.H. (1981). The *Saccharomyces cerevisiae* cell cycle. In: The Molecular Biology of the Yeast *Saccharomyces*, Life Cycle and Inheritance, ed. J.N. Strathern, E.W. Jones, and J.R. Broach, Cold Spring Harbor, NY: Cold Spring Harbor Laboratory Press, 97–142.

Pringle, J.R., Lillie, S.H., Adams, A.E.M., Jacobs, C.W., Haarer, B.K., Coleman, K.G., Robinson, J.S., Bloom, L., and Preston, R.A. (1986). Cellular morphogenesis in the yeast cell cycle. In: Yeast Cell Biology, ed. J. Hicks, New York: Alan R. Liss, 47–80.

Rebecchi, M.J., and Scarlata, S. (1998). Pleckstrin homology domains: a common fold with diverse functions. Annu. Rev. Biophys. Biomol. Struct. *27*, 503–528.

Richman, T.J., Sawyer, M.M., and Johnson, D.I. (1999). The Cdc42p GTPase is involved in a G_2/M morphogenetic checkpoint regulating the apical-isotropic switch and nuclear division in yeast. J. Biol. Chem. *274*, 16861–16870.

Riles, L., Dutchik, J.E., Baktha, A., McCauley, B.K., Thayer, B.C., Leckie, M.P., Braden, V.V., Depke, J.E., and Olson, M.V. (1993). Physical maps of the six smallest chromosomes of *Saccharomyces cerevisiae* at a resolution of 2.6 kb pairs. Genetics *134*, 81–150.

Rose, M.D., and Broach, J.R. (1991). Cloning genes by complementation in yeast. Methods Enzymol. *194*, 195–230.

Sambrook, J., Fritsch, E.F., and Maniatis, T. (1989). Molecular Cloning: A Laboratory Manual, Cold Spring Harbor, NY: Cold Spring Harbor Laboratory Press.

Sandbaken, M.G., and Culbertson, M.R. (1988). Mutations in elongation factor EF1-α affect the frequency of frameshifting and amino acid misincorporation in *Saccharomyces cerevisiae*. Genetics *120,* 923–934.

Sells, M.A., and Chernoff, J. (1997). Emerging from the Pak: the p21-activated protein kinase family. Trends Cell Biol. *7*, 162–167.

Shannon, K.B., and Li, R. (1999). The multiple roles of Cyk1p in the assembly and function of the actomyosin ring in budding yeast. Mol. Biol. Cell *10*, 283–296.

Sikorski, R.S., and Boeke, J.D. (1991). In vitro mutagenesis and plasmid shuffling: from cloned gene to mutant yeast. Methods Enzymol. *194,* 302–318.

Sikorski, R.S., and Hieter, P. (1989). A system of shuttle vectors and yeast host strains designed for efficient manipulation of DNA in *Saccharomyces cerevisiae*. Genetics *122,* 19–27.

Simon, M.-N., De Virgilio, C., Souza, B., Pringle, J.R., Abo, A., and Reed, S.I. (1995). Role for the Rho-family GTPase Cdc42 in yeast mating-pheromone signal pathway. Nature *376*, 702–705.

Sloat, B.F., Adams, A., and Pringle, J.R. (1981). Roles of the *CDC24* gene product in cellular morphogenesis during the *Saccharomyces cerevisiae* cell cycle. J. Cell Biol. *89*, 395–405.

Soisson, S.M., Nimnual, A.S., Uy, M., Bar-Sagi, D., and Kuriyan, J. (1998). Crystal structure of the Dbl and pleckstrin homology domains from the human Son of Sevenless protein. Cell *95*, 259–268.

Stevenson, B.J., Ferguson, B., De Virgilio, C., Bi, E., Pringle, J.R., Ammerer, G., and Sprague, G.F., Jr. (1995). Mutation of *RGA1*, which encodes a putative GTPase-activating protein for the polarity-establishment protein Cdc42p, activates the pheromone-response pathway in the yeast *Saccharomyces cerevisiae*. Genes Dev. *9*, 2949–2963.

Tanaka, K., Matsumoto, K., and Toh-e, A. (1989). *IRA1*, an inhibitory regulator of the *RAS*-cyclic AMP pathway in *Saccharomyces cerevisiae*. Mol. Cell. Biol. *9,* 757–768.

Tanaka, K., Nakafuku, M., Satoh, T., Marshall, M.S., Gibbs, J.B., Matsumoto, K., Kaziro, Y., and Toh-e, A. (1990a). *S. cerevisiae* genes *IRA1* and *IRA2* encode proteins that may be functionally equivalent to mammalian *ras* GTPase activating protein. Cell *60*, 803–807.

Tanaka, K., Nakafuku, M., Tamanoi, F., Kaziro, Y., Matsumoto, K., and Toh-e, A. (1990b). *IRA2*, a second gene of *Saccharomyces cerevisiae* that encodes a protein with a domain homologous to mammalian *ras* GTPase-activating protein. Mol. Cell. Biol. *10*, 4303–4313.

Tanaka, K., and Takai, Y. (1998). Control of reorganization of the actin cytoskeleton by Rho family small GTP-binding proteins in yeast. Curr. Opin. Cell Biol. *10*, 112–116.

Tyers, M., Tokiwa, G., and Futcher, B. (1993). Comparison of the *Saccharomyces cerevisiae* G_1 cyclins: Cln3 may be an upstream activator of Cln1, Cln2 and other cyclins. EMBO J. *12*, 1955–1968.

Umikawa, M., Tanaka, K., Kamei, T., Shimizu, K., Imamura, H., Sasaki, T., and Takai, Y. (1998). Interaction of Rho1p target Bni1p with F-actin-binding elongation factor 1α: implication in Rho1p-regulated reorganization of the actin cytoskeleton in *Saccharomyces cerevisiae.* Oncogene *16,* 2011–2016.

Valencia, A., Chardin, P., Wittinghofer, A., and Sander, C. (1991). The *ras* protein family: evolutionary tree and role of conserved amino acids. Biochemistry *30*, 4637–4647.

Van Aelst, L., and D'Souza-Schorey, C. (1997). Rho GTPases and signaling networks. Genes Dev. *11*, 2295–2322.

Wasserman, S. (1998). FH proteins as cytoskeletal organizers. Trends Cell Biol. *8*, 111–115.

Whitehead, I.P., Campbell, S., Rossman, K.L., and Der, C.J. (1997). Dbl family proteins. Biochim. Biophys. Acta *1332*, F1–F23.

Xu, X.-Z.S., Wes, P.D., Chen, H., Li, H.-S., Yu, M., Morgan, S., Liu, Y., and Montell, C. (1998). Retinal targets for calmodulin include proteins implicated in synaptic transmission. J. Biol. Chem. *273*, 31297–31307.

Yang, S., Ayscough, K.R., and Drubin, D.G. (1997). A role for the actin cytoskeleton of *Saccharomyces cerevisiae* in bipolar bud-site selection. J. Cell Biol. *136*, 111–123.

Zahner, J.E., Harkins, H.A., and Pringle, J.R. (1996). Genetic analysis of the bipolar pattern of bud site selection in the yeast *Saccharomyces cerevisiae*. Mol. Cell. Biol. *16*, 1857–1870.

Zhang, S.-D., Kassis, J., Olde, B., Mellerick, D.M., and Odenwald, W.F. (1996). Pollux, a novel *Drosophila* adhesion molecule, belongs to a family of proteins expressed in plants, yeast, nematodes, and man. Genes Dev. *10*, 1108–1119.

Zhao, Z.-S., Leung, T., Manser, E., and Lim, L. (1995). Pheromone signaling in *Saccharomyces cerevisiae* requires the small GTP-binding protein Cdc42p and its activator *CDC24*. Mol. Cell. Biol. *15,* 5246–5257.

Zheng, Y., Bagrodia, S., and Cerione, R.A. (1994a). Activation of phosphoinositide 3-kinase activity by Cdc42Hs binding to p85*. J. Biol. Chem. *269*, 18727–18730.

Zheng, Y., Bender, A., and Cerione, R.A. (1995). Interactions among proteins involved in bud-site selection and bud-site assembly in *Saccharomyces cerevisiae.* J. Biol. Chem. *270,* 626–630.

Zheng, Y., Cerione, R., and Bender, A. (1994b). Control of the yeast bud-site assembly GTPase Cdc42. Catalysis of guanine nucleotide exchange by Cdc24 and stimulation of GTPase activity by Bem3. J. Biol. Chem. *269*, 2369–2372.

Ziman, M., O'Brien, J.M., Ouellette, L.A., Church, W.R., and Johnson, D.I. (1991). Mutational analysis of *CDC42Sc*, a *Saccharomyces cerevisiae* gene that encodes a putative GTP-binding protein involved in the control of cell polarity. Mol. Cell. Biol. *11*, 3537–3544.

Ziman, M., Preuss, D., Mulholland, J., O'Brien, J.M., Botstein, D., and Johnson, D.I. (1993). Subcellular localization of Cdc42p, a *Saccharomyces cerevisiae* GTP-binding protein involved in the control of cell polarity. Mol. Biol. Cell *4*, 1307–1316.